sciendo
Austrian Journal of Earth Sciences Vienna 2023 Volume 116 17 - 38 DOI: 10.17738/ajes.2023.0002

Old orogen – young topography: Evidence for relief rejuvenation in the Bohemian Massif

Klaus Wetzlinger[1], Jörg Robl[1*], Moritz Liebl[1], Fabian Dremel[1], Kurt Stüwe[2] and Christoph von Hagke[1]

[1)] Department of Environment and Biodiversity, Division of Geology and Physical Geography, University of Salzburg, 5020 Salzburg, Austria

[2)] Institute for Earth Sciences, University of Graz, 8020 Graz, Austria

[*)] Corresponding author: Jörg Robl

KEYWORDS: landscape evolution. relief rejuvenation, Bohemian Massif, divide migration, fluvial erosion

Abstract

The Bohemian Massif is the relic of a major Paleozoic mountain range that is known to have exhumed and its surface levelled in the Permian, but its Neogene landscape evolution is largely unconstrained. The landscape is characterized by rolling hills and extended planation surfaces above an elevation of about 500 m. However, at lower elevations deeply incised gorges confined by steep hillslopes are abundant and contrast impressively with the low relief landscapes above. Rivers with a bimodal morphology (i.e. steep at lower elevations and gentle at higher elevations) drain either to the north into the Vltava (Moldau) River or to the south into the Danube River. Hence, a continental drainage divide runs through the Bohemian Massif. Here, we quantify spatial characteristics of the Bohemian Massif landforms by computing landscape metrics like steepness index or geophysical relief derived from digital elevation models. From this we infer temporal change of the landscape in the past and predict them for the future evolution of the region.

We show that the landscape is characterized by out-of-equilibrium river profiles with knickpoints abundantly at elevations between 450 m and 550 m separating steep channel segments at lower elevations from less steep channels at higher elevations. Hypsometric maxima at or close above knickpoint elevations, along with high and low values in geophysical relief as indicator for the degree of fluvial landscape dissection downstream and upstream of major knickpoints, support the idea of landscape bimodality. Furthermore, we find a distinct drainage divide asymmetry, which causes the reorganization of the drainage network of the region. Across-divide gradients in channel steepness predict the northward migration of the Danube-Vltava drainage divide including growth and shrinkage of tributary catchments, thus controlling changes in the Central European drainage pattern.

All aspects suggest that the region experienced relief rejuvenation during the last few million years. We suggest that this relief rejuvenation is related to the inversion of the Molasse basin with a long wavelength rock uplift pattern and low uplift rates. Vertical motion of crustal blocks at discrete faults may locally affect the uplift pattern. However, the contrasting bedrock properties between the sedimentary cover (Molasse sediments) and the crystalline basement (Bohemian Massif) cause substantial differences in erosion rate and are thus the superior control on the topographic variations of the entire region.

1. Introduction

Most mountain ranges with peak elevations exceeding three kilometers such as the European Alps, the Himalaya or the Andes evolve at convergent plate boundaries, where crustal shortening and thickening drive isostatic uplift, which eventually leads to high topography (e.g. England and Houseman, 1986; Robl and Stüwe, 2005a, b). However, several regions on Earth, where these mountain-building processes ceased a long time ago, indicate that high topography can be formed or at least maintained in absence of orogenic processes at plate boundaries. Prominent examples for such regions are the Appalachian mountains (Miller et al., 2013; Dethier et al., 2014), the western Indian margin (Mandal et al., 2015), or the Massif Central (Olivetti et al., 2016). Another area with significant topography in an ancient mountain range is the Bohemian Massif (BM).

The BM represents the remnant of a major Paleozoic mountain range, which originally formed during the Variscan orogeny more than 300 Myrs ago (e.g. O'Brien and Carswell, 1993; Kroner and Romer, 2013; Franke, 2014). However, the initial topography, which formed at a convergent plate boundary, was largely eroded and leveled in the Permian (Hejl et al., 1997; Hejl et al., 2003; Bourgeois et al., 2007; Ziegler and Dèzes, 2007; Lange et al., 2008; Danišík et al., 2010) but experienced several phases of uplift and subsidence hereinafter (for details see Ziegler and Dèzes, 2007 and references therein). Apatite fission-track ages indicate a slow but steady exhumation in the Early Cretaceous (Hejl et al., 2003; Vamvaka et al., 2014) and a reburial in the Late Cretaceous (Hejl et al., 2003; Wessely, 2006). For the late Cenozoic, different mechanisms such as plume-related delamination of the mantle-lithosphere or lithospheric unloading triggering a renewed uplift event are discussed. This uplift appears to have affected large parts of the Eastern Alps, the Molasse Basin and the BM (Genser et al., 2007; Gusterhuber et al., 2012; Baran et al., 2014), but its topographic expression has only been described in detail for some areas at the eastern fringe of the Alps (Robl et al., 2008a; Wagner et al., 2010; Wagner et al., 2011; Legrain et al., 2014; Legrain et al., 2015; Robl et al., 2015; Stüwe and Hohmann, 2021), for the Hausruck – Kobernaußerwald region in the Molasse Basin (Baumann et al., 2018) and for the fault bounded Budějovice basin (Popotnig et al., 2013) and the sudetic marginal fault (Badura et al., 2007) in the Bohemian Massif.

In this study we test the hypothesis of relief rejuvenation and related drainage network reorganization in the southern BM by analyzing properties of the drainage system and related hillslopes. Therefore, we employ a series of morphometric analyses such as hypsometric curves and integrals, longitudinal channel profiles, normalized steepness index (k_{sn}) and χ mapping, slope-elevation distributions, and geophysical relief along rivers and torrents.

2. Geological and geomorphological background

The BM covers large parts of the Czech Republic, parts of eastern Germany, southern Poland and northern Austria. Representing a classical "Mittelgebirge", the highest elevations hardly exceed 1400 m above sea level (a.s.l.). Consistently, the landscape of the study area is predominantly characterized by gentle topographic features such as rolling hills and wide valleys. However, these topographic observations only apply for the central higher part of the mountain range, while the landscape close to the receiving streams is heavily dissected with steep channels flowing in narrow gorges. The continental divide follows the crest of the BM and separates tributaries of the Danube River from those of the Vltava (Moldau) River. As we aim to predict aspects of the Central European drainage reorganization we focus on this area around the continental divide in the southern BM. The Black Sea and the North Sea represent the base levels of the Danube and the Elbe drainage system with the Vltava as its largest tributary. According to the large-scale topographic gradient, the tributaries of the Danube R. and the Vltava River drain roughly towards south and north. The southern fringe of the BM is covered by sediments of the Northern Neogene Alpine Foreland Basin. The Danube River follows the spur of the BM, erodes the sedimentary cover but also incises the crystalline basement. In the latter case the Danube valley forms deep gorges. Neogene sediments occur also north of the continental drainage divide (e.g. Budweis and Trebon basins) in the Vltava catchment (Cháb et al., 2007; Ziegler and Dèzes, 2007; Homolová et al., 2012; Tschegg and Decker, 2013). The southern BM is dissected by a conjugate system of NW-SE striking dextral and NE-SW striking sinistral strike slip shear zones (e.g. Lenhardt et al., 2007). The orientations of these tectonic faults correspond roughly to directions of streams, which deviate distinctly from the overall topographic gradient. Even the Danube River follows one of these NW-SE striking faults tens of kilometers.

Geologically, the BM formed during the Variscan Orogeny with the so called Moldanubian zone covering the southeastern part of the orogen (Kossmat, 1927) (Fig. 2). The Moldanubian Zone is subdivided into the Moldanubian Nappes (Gföhl Unit, the Ostrong Unit and the Drosendorf Unit), the Bavaricum, and the South Bohemian Batholith (Linner et al., 2011). The Bavaricum forms an independent tectonic unit, which is distinguished from Moldanubian nappes on the basis of deformation style and metamorphic conditions (Fuchs and Matura, 1976; Finger et al., 2007). In the late stage of Variscan orogeny (between 340 and 300 Myrs), both units, the Moldanubian Nappes and the Bavaricum were intruded by a large amount of syn- and posttectonic granitic rocks, which form in their entirety the South Bohemian Batholith (Finger et al., 2009; Linner et al., 2011).

Conjugate crustal scale strike slip zones are connected with the asymmetric exhumation of the southern BM in the late stages of the Variscan orogeny (Brandmayr et al., 1999) (Fig. 2). In the western part, these are the NW-SE

striking Pfahl and Danube shear zones, and in the eastern part, these are the NE-SW striking Rodl-Kaplice, Karlstifter and Vitis shear zones (and the Diendorf-Boskovice fault east of the study area). Due to a regional Miocene-Pliocene uplift event pre-existing crustal discontinuities within the BM were reactivated (Ziegler and Dèzes, 2007). The European Cenozoic Rift System (ECRIS) is an active fault system, which cause exhumation rates of up to 1.75 mm/yr in Variscan Massifs such as the Armorican Massif, the Massif Central, the Rhenish Massif and the northern parts of the BM (Ziegler and Dèzes, 2007). Clearly, faults dissected the bedrock of the investigated region and force rivers to follow the fault traces even if they deviate significantly from the general topographic gradient (Figs. 1, 2).

2.1 Geomorphological history

Little is known about the topography of the Bohemian Massif during the Variscan orogeny. However, Franke (2014) suggested that the mountain height of the Variscan orogen was strongly limited by its low mechanical strength. Direct evidence for the geomorphological evolution of the Variscan Massif dates back to the Late Carboniferous and Early Permian, where a Molasse basin formed (e.g. Schäfer, 1989). In the Late Permian, planation surfaces within the BM evolved due to a major erosional phase (Balatka and Kalvoda, 2008). Carboniferous and Permian sediments are also known from the eastern end of the BM (Wessely, 2006). However, there is a lack of geomorphological information from the Triassic to the Late Cretaceous (Pánek and Kapustová, 2016). In the Late Cretaceous a widespread marine transgression took place as indicated by apatite fission track ages evidencing for a sedimentary reburial of about one kilometer (Hejl et al., 2003; Vamvaka et al., 2014). Thermochronological data from planation surfaces at the Karkonosze Mts. (NE of the Czech Republic) indicate that they were exhumed in the Late Cretaceous after the removal of Cretaceous sediments (Danišík et al., 2010). Nevertheless, the exhumation history of other domains of the BM is still unknown (Pánek and Kapustová, 2016). In the Paleogene and Neogene, fluctuating climatic conditions in combination with neotectonic activity controlled the topographic evolution (Ziegler and Dèzes, 2007; Pánek and Kapustová, 2016). Throughout the Pleistocene deep fluvial incision and the formation of canyon-like valleys (e.g. Vltava R.) was interpreted as the expression of intense uplift at that time (Pánek and Kapustová, 2016). Today, the topography of the BM is characterized by extended planation surfaces at higher elevations, which are peripherally dissected by deep gorges. The river morphology dramatically changes from meandering, low gradient channels at the central parts of the plateau to high gradient river segments at the plateau rims close to the receiving streams. T-shaped river junctions, where two rivers drain in the same valley but in opposite direction and turn their flow direction at the confluence point by about 90°, are observed (Fig. 1, Große Mühl). Such distinct flow direction changes in concert with wind gaps are often attributed to river piracy events (Robl et al., 2008b; Robl et al., 2017a) and hence may evidence for recent drainage network reorganization in the BM.

2.2 Drainage system

Two major drainage systems, the Danube drainage system in the south and the Labe (Elbe) drainage system (with the Vltava as its largest tributary) in the north controlled the morphological evolution of the BM. The two catchments are separated by an E-W striking continental drainage divide that is also known as the European watershed. Tyráček and Havlíček (2009) reconstructed the Miocene drainage pattern within the Czech Republic (and hence predominantly north of the continental divide). They suggested that the upper part of the Labe catchment drained eastwards to the Paratethys, and that rivers from Western Bohemia terminated in Neogene freshwater lakes situated in the northwest of the country. In their reconstruction, the southern part of the Vltava catchment drained southwards to the Alpine foreland.

Currently the Danube River follows the southern spur of the BM. Its riverbed consists either of sediments of the Molasse Basin (also Quaternary sediments), or of crystalline rocks of the BM. While the Danube valley is wide and features gentle valley flanks in sections draining in the Molasse Basin, deep gorges with steep valley flanks are characteristic for the crystalline bedrock of the BM indicating the strong contrast in bedrock erodibility of the two units. The flow direction of the Danube River changed several times since the Oligocene (e.g. Kuhlemann et al., 2006). Until the end of Early Miocene, the Danube and all major rivers draining the northern side of the Eastern Alps terminated in the Molasse Sea. With the siltation of the Molasse Sea in the Mid-Miocene, the Danube drained towards the west, before basin inversion, uplift and tilting of the Alpine foreland resulted in the present flow (e.g. Kuhlemann et al., 2006). From 11 Ma on, the Danube drainage system started to drain the Molasse Basin from west to east (Mackenbach, 1984). The today's course of the Danube River developed from this early river system in the Pleistocene (Hantke, 1993).

The Vltava River is a tributary of the Elbe River and the longest river within the Czech Republic. The Vltava River originates in the South Bohemia Region near Kvilda (southwestern part of the Czech Republic). At Melník the Vltava River confluences with the Elbe River, which eventually drains into the North Sea. Similar to the Danube River, the evolution of the modern Vltava River began in the Early Pleistocene and is controlled by neotectonic uplift and climate change (Pánek and Kapustová, 2016). Interestingly, the erosion rate was found to be dependent on changes of climatic conditions throughout the Pleistocene with Middle Pleistocene humid interglacial/interstadial conditions leading to intense fluvial incision [60-80 cm/kyrs] and subsequently to the formation of

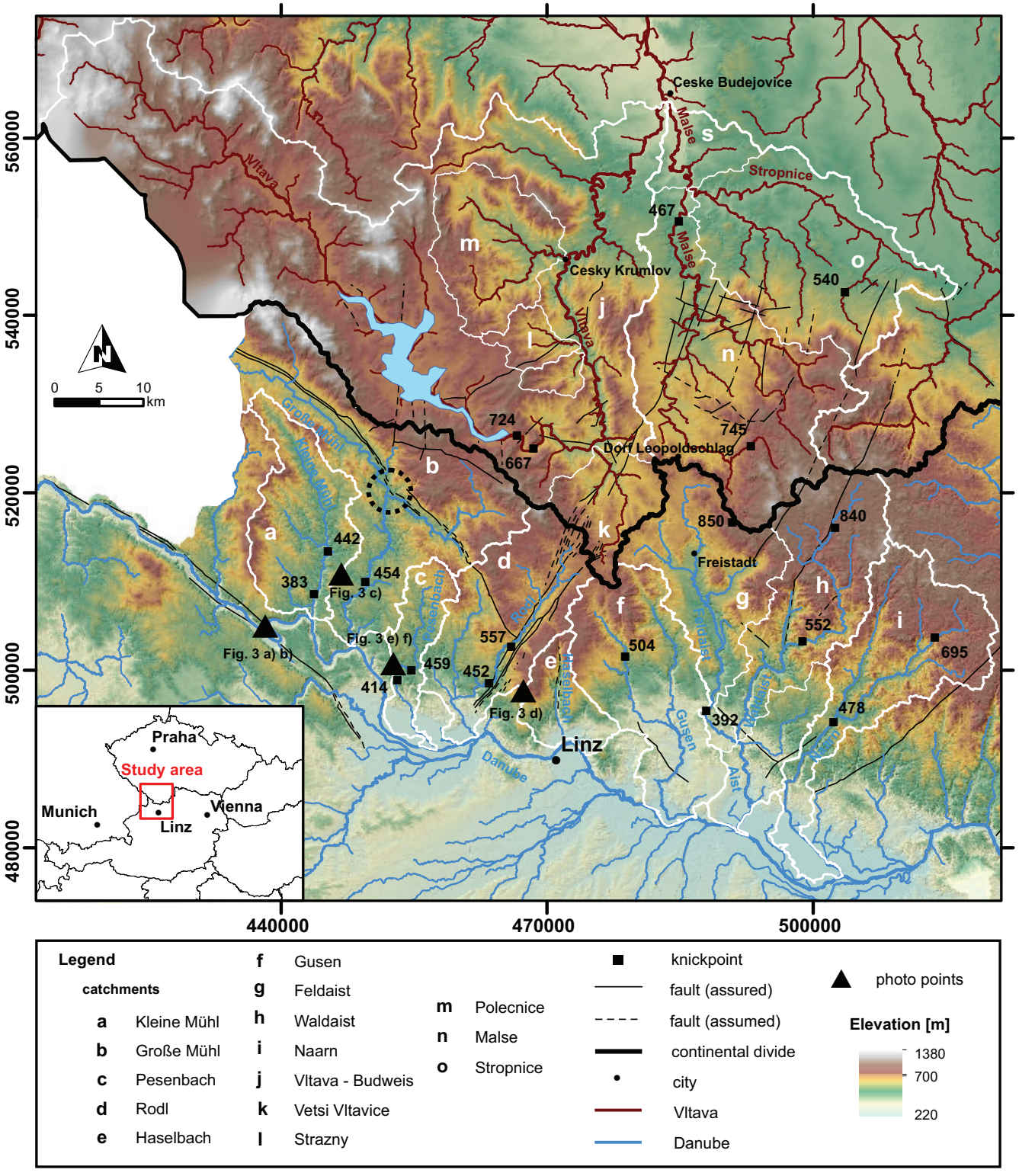

Figure 1: Topographic map of the study area. The continental divide (thick black line) separates the Danube (blue) from the Vltava (red) drainage system. Drainage divides of tributaries are indicated by white lines. Major faults (thin black lines), knickpoints in channels (black squares) and location of photo points (black triangles, see Fig. 3) are shown. The black circle with dashed line indicates the position of the T-shaped river junction.

deep valleys of the Vltava River (Balatka and Kalvoda, 2008; Pánek and Kapustová, 2016).

3. Data and Methods

The topographic analyses are performed on digital elevation models (DEM) for Austria and the Czech Republic with a spatial resolution of 10 m. To merge the two DEMs, they were reprojected to a common coordinate system (MGI Austria Lambert, 130 EPSG:31297). ArcMap 10.6.1 (ESRI Inc.) was used for the generation of base maps. Morphological analyses of the stream network were performed with standard approaches as implemented in TopoToolbox (Schwanghart and Kuhn, 2010; Schwanghart and Scherler, 2014) and a tool provided by Hergarten et al. (2016) for χ mapping. In particular, the following analyses are applied.

3.1 Hypsometric analysis and geophysical relief

Hypsometric curves and the hypsometric integral (the area under the hypsometric curve) are used to indicate different topographic states. For example, it is known that hypsometric integrals close to 0.5 along with S-shaped hypsometric curves are characteristic for a topographic steady state (Strahler, 1952; Ohmori, 1993; Cheng et al., 2012). As such, the hypsometric curve and its integral (*HI*) allows the comparison of catchments that differ in size and catchment relief (i.e. elevation difference between outlet and the highest mountain peak of the catchment) (Strahler, 1952). To achieve this, the normalized cumulative distribution of area against elevation is applied. To calculate *HI*, we determine the area fractions for 50 m wide elevation bins, sum them up, and then divide them by the number of bins.

The geophysical relief is a diagnostic indicator to estimate the mean erosion rate (e.g. Champagnac et al., 2007). It is computed by subtracting the current topography from a surface which connects summit flats at similar elevations at a given circular moving window (Small and Anderson, 1998). A window size of 1000 m was chosen for the calculation of the geophysical relief. The comparison with the longitudinal river profiles of the studied catchments aimed to reveal differences in geophysical relief up- and downstream of knickpoints.

3.2 Longitudinal river profiles

Longitudinal channel profiles are used because it is well known that they are indicative for tectonic and climatic conditions (e.g. Wobus et al., 2006; Kirby and Whipple, 2012; Robl et al., 2017b). The morphological analysis of the drainage system was performed with TopoToolbox (Schwanghart and Scherler, 2014). Channel segments and contributing drainage area are computed by a standard single flow algorithm (D8) (O'Callaghan and Mark, 1984). The threshold drainage area for extraction of the drainage network was set to 1 km^2. To obtain channel profiles, we started at given outflow coordinates and extracted the elevation values along the calculated flow path in upstream direction. Knickpoints are defined by sharp convex sections in longitudinal channel profiles and are detected by fitting steady state profiles to measured channel segments by applying the "knickpointfinder" function of Topotoolbox (Schwanghart and Scherler, 2014, 2017). The default threshold value for the vertical offset of 20 m between measured and modelled profiles is used and hence only major knickpoints are considered.

For the interpretation of channel profiles, we have extracted the steepness index *k*s from the fluvial channels to compare the ability of the rivers to incise into the bedrock. The steepness index is typically expressed as $k_s = A^{-\theta}(\mathrm{d}H/\mathrm{d}x)$ which is also known as Flint's law (Flint, 1974). In this expression, A is the contributing drainage area (as a proxy for the discharge of a river), θ is the concavity index, H is the elevation and x marks the longitudinal coordinate increasing upstream from the outlet ($x = 0$). Hence, $\mathrm{d}H/\mathrm{d}x$ represents the channel slope. For graded rivers in geomorphic steady state (rivers that erode everywhere at the same rate under uniform conditions) in detachment limited fluvial regimes, *k*s is constant along a river and is proportional to erosion rate. This allows a direct comparison of rivers with catchment sizes that differ by several orders of magnitude. As k_s and θ are strongly correlated, a direct comparison of the channel steepness between individual rivers require the definition of a reference concavity index (θ_{ref}). Based on the analysis of longitudinal river profiles most of the recent studies apply $\theta_{ref} = 0.45$ or $\theta_{ref} = 0.5$ (Hack, 1957; Whipple, 2004; Wobus et al., 2006; Lague, 2014; Robl et al., 2017a; Robl et al., 2017b). In this study we use $\theta_{ref} = 0.5$. Then the steepness index is referred to as normalized steepness index k_{sn} with the unit meters. Assuming a uniform uplift rate, erodibility, and climate, fluvial landscapes exhibit spatially constant k_{sn} values. Therefore, any deviations from such an equilibrium state (knickpoints) should be detectable in a k_{sn} map and can be interpreted in terms of spatial or temporal changes in substrate properties, climatic conditioning, or tectonic forcing.

3.3 χ mapping

A rather new approach to the analysis of bedrock river profiles is the χ transformation (Perron and Royden, 2013; Royden and Taylor Perron, 2013). It is based on the integration of the steady-state form (where the uplift rate U equals the erosion rate E) of the stream power equation (Howard et al., 1994; Lague, 2014), where the change in surface elevation of time t is given by:

$$\frac{\partial H}{\partial t} = U - E \quad \text{with:} \quad E = KA^m \left(\frac{\partial H}{\partial x}\right)^n \tag{1}$$

The erosional efficiency is represented by *K,* which is a lumped parameter including the resistance of the

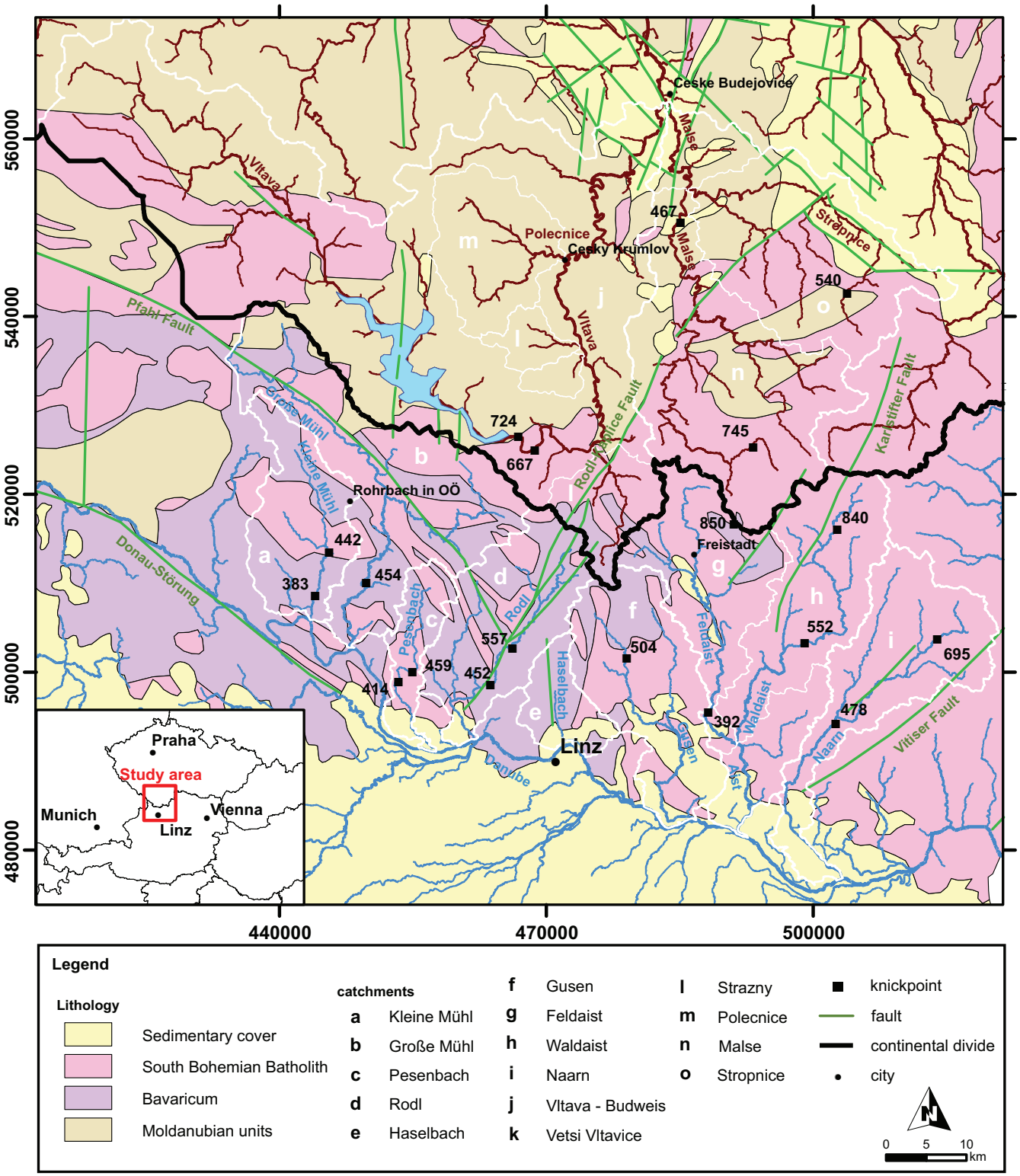

Figure 2: Simplified geological map of the study area based on the geological maps of the Geologische Bundesanstalt (GBA): „Geologische Übersichtskarte der Republik Österreich 1:1 500 000" (Egger et al., 1999) and „Tektonische Übersichtskarte 1:100 000 (Beilage zur Geologischen Karte von Oberösterreich 1:200 000" (Linner et al., 2011)).

bedrock to erosion but also climatic properties such as precipitation rate gradients or flood frequency, or sediment transport processes (e.g. Harel et al., 2016). The exponents *m* and *n* give the contribution of contributing drainage area and channel slope to river incision. The curvature of the channel profile results from an increase in contributing drainage area with downstream distance. This makes it difficult to detect spatial or temporal changes in uplift rate from the geometry of the fluvial channel. Transforming the longitudinal coordinate *x* to a new coordinate χ eliminates the curvature of the river profile introduced by the contributing drainage area and facilitates the detection of tectonic, lithologic, and climatic signals and transient states in river profiles with varying catchment sizes (Perron and Royden, 2013; Royden and Taylor Perron, 2013). The contributing drainage area can be eliminated if the transformation meets the following criterion:

$$\frac{\partial x}{\partial \chi} = \left(\frac{A}{A_0}\right)^{\theta_{ref}}, \tag{2}$$

with

$$\chi = \int_{x_0}^{x} \left(\frac{A}{A_0}\right)^{-\theta_{ref}} dx \tag{3}$$

The quantity χ is an integral function of the position in the channel network starting from an arbitrary given reference point x_0. The arbitrary reference catchment size A_0 gives χ dimensions of length, and only affects the absolute scale of the values. The erosion rate can then be written as follows:

$$E = K \left(\frac{\partial H}{\partial \chi}\right)^{n}. \tag{4}$$

Assuming $n = 1$ in Eq. 4, one can easily deduce that χ serves as a metric for the steady-state elevation of a channel at location *x*. Assuming uniform tectonic conditions and substrate properties, steady-state channel profiles turn into straight lines by plotting χ against *H*. As can easily be seen, the slope of the channel profile is proportional to the normalized steepness index (k_{sn}). If the elevation drop of rivers on both sides of a common drainage divide is the same, which is achieved by defining the same base-level elevation for the χ integration, rivers with smaller χ at the common divide are on average steeper (higher k_{sn}) than those with larger χ (Perron and Royden, 2013). This is exploited by the so called χ mapping where the drainage network is color-coded for χ and across divide differences in mean channel steepness and hence erosion rate (assuming uniform conditions) can be directly investigated (Willett et al., 2014).

χ values were computed for all channels with a contributing drainage area $A_0 = 1$ km^2, $\theta = 0.5$ and different base levels $H(x_0) = 150$ and 400 m. The chosen baselevel determines the considered area computing χ. A lower base level means a larger distance from the base level to the investigated drainage divide and thus larger catchments are considered. As a consequence, low base levels will represent a large-scale pattern of χ including far field effects, while a high base level shows the χ pattern at the tributary scale (for more details see Trost et al., 2020; Fan et al., 2021).

3.4 Slope-elevation distribution

We examine the relationship between slope distribution and elevation, a method that has been used in both fluvial and glacial terrain to characterize the topographic state of a landscape (Kühni and Pfiffner, 2001; Hergarten et al., 2010; Robl et al., 2015; Liebl et al., 2021). Slopes are calculated for each cell by a standard single flow algorithm (D8). The slopes are following the steepest descent along the flow paths. The slope data are classified into 50 m wide elevation bins. For each bin the mean and percentiles (P25, P50, and P75) are calculated. The relative frequency distribution of slope values is assessed using 0.02 m/m wide slope bins to provide a graphical representation of the slope distribution per elevation bin (Robl et al., 2015).

4. Results

Field observations in concert with morphological analyses reveal distinct topographic differences between the Danube and Vltava drainage systems but also differences within the respective catchments. Here, a clear elevation dependence of the topographic features is particularly evident, with steep landforms occurring near the receiving streams (e.g. Danube) and less steep ones at higher elevations.

4.1 Field observations

At lower elevations and here in particular at the southern flank of the BM close to the Danube the landscape is characterized by high amplitude, low wavelength features. Near Schlögen, the Danube has carved a deep gorge with steep hillslopes into the crystalline bedrock of the BM. Figures 3a and 3b show the so called Schlögener Schlingen with steep ~200 m high valley flanks and flat hilltops that occur roughly at the same altitude (~ 500 m a.s.l.). At the hilltops Quaternary sediments consisting of fluvial gravels from the former Danube are preserved. At elevations above 500 m a.s.l., the landscape is characterized by long wavelength, low amplitude landforms such as smooth hills separated by abundantly meandering rivers with wide and flat valley floors. Towards the north, the elevation increases progressively (Fig. 3c). However, Fig. 3d shows that there is more than one distinct level of planation surfaces. The transition between the low relief landscapes at higher elevations (≥ 500 m a.s.l.) and the current base level of the Danube (~ 260 m a.s.l.) features

Figure 3: Field observations at the southern flank of the BM. Landscape impressions around the Schlögener Schlingen: (a) View to the W, (b) View to the E, (c) View to the N, (d) View to the SE. For exact location see Fig. 1. (e) Downstream shot of Pesenbach. (~ 340 m a.s.l. / South 160°), (f) Segment of Pesenbach located downstream of the knickpoint. The picture was taken at an elevation of ~ 410 m a.s.l..

a series of north-south running gorges with high channel gradients, very high local relief and hillslopes with abundant evidence of rapid mass movements (Fig. 3e, f). Knickpoints in rivers occur at elevations between 400 and 500 m a.s.l. and separate steep channel segments downstream from less steep channel segments upstream. The same applies to breaks in slope, which separate low gradient hillslopes roughly above 500 m a.s.l. from steep hillslopes below. The Pesenbach, a tributary to the Danube, is exemplary for these north-south flowing rivers (Fig. 1, 3e, f). Starting at its confluence with the Danube and following the Pesenbach upstream, the river features very low channel gradients for about 10 km. However, further upstream the channel steepness increases substantially. This river segment is characterized by a narrow, 5 to 10 m wide bedrock channel (Fig. 3e) with up to 50 m, almost vertical valley flanks. Boulders of various sizes as relics of rock falls at the valley floors, small steps with little waterfalls and pools, and blank bedrock sections as evidence for hillslope processes (e.g. rockfalls) and fluvial incision are abundant features of this river segment (Fig. 3f). Upstream of this steep and rather short segment, a several tens of kilometer long river segment follows, which is well in line with smooth landscape of the BM above an altitude of about 500 m a.s.l.. Low channel gradients, gentle valley flanks and a low relief characterize this river landscape.

4.2 Tectonic Lineaments and drainage network

Within the study area NW-SE striking dextral and NE-SW striking sinistral systems of conjugate strike slip shear zones are found (Fig. 2). From west to east these are the Danube shear zone and the Pfahl shear zone, both northwest-southeast trending shear zones, and the Rodl shear zone, the Karlstift shear zone and the Vitis shear zone, all northeast-southwest trending shear zones. Further in the east, outside the investigated area, there is the Diendorf shear zone, which completes the conjugate strike slip shear zone system in the southern BM.

Comparing the principal direction of streams of the study area with the orientation of tectonic lineaments, we observe a concordance of flow direction and fault orientation for river segments of several tens of kilometers. The Danube at the western part of the study area as well as the upper reach of the Große Mühl follow northwest-southeast trending shear zones (Danube shear zone and Pfahl shear zone). Interestingly, further in the north the headwaters of the Vltava River are parallel to the mentioned shear zones downstream to the point where the conjugated northeast-southwest trending Rodl shear zone intersect the river course. The flow direction of the river Rodl and of the upper reach of the river Malše is consistent with the orientation of the Rodl shear zone. Further in the east, the orientation of the Karlstift and the Vitis shear zone is found only vaguely, if at all, in the orientation of the river segments. However, the drainage network within the whole study area features predominantly northwest-southeast or northeast-southwest trending channels. Even the continental divide separating the Danube from the Vltava drainage system is in line with the orientation of the dominant fault systems of the region. In the west, the watershed strikes northwest-southeast and changes its direction to northeast-southwest approximately at the intersection with the Rodl shear zone.

4.3 Hypsometric analysis

The occurrence of spacious planation surfaces at mid- and high elevation and steep channels and hillslopes close to the base level of the receiving streams are reflected in a characteristic pattern in the hypsometry of the investigated catchments (Figs. 4, 5). The three westernmost tributaries of the Danube that are characterized by similar channel profiles, show also similar hypsometric properties (Fig. 4a-c). The areal maxima occur at an elevation of about 500 m a.s.l. and hence at the position of the major knickpoints in channels that separate steep from less steep channel segments in downstream and upstream direction, respectively. Such a hypsometry causes a S-shaped hypsometric curve with hypsometric integrals of about 0.5. Only the Große Mühl features a distinctly lower hypsometric integral, which is due to the influence of the peak elevation on the analysis. The highest mountain peak of the study area is located in the Große Mühl catchment (see Fig. 1). The Rodl River with its main course following the Rodl fault also shows a pronounced hypsometric maximum but at about 700 m a.s.l.. Further east, the Haselbach and the river Gusen do not show pronounced hypsometric maxima but a similar proportion of area from the base level to the summit areas, which is reflected by a fairly linear hypsometric curve. While the Feldaist catchment again shows similar hypsometric properties than the four westernmost catchments with an S-shaped hypsometric curve, the hypsometric maxima of the two easternmost catchments (i.e. the rivers Waldeist and Naarn) are located at high elevations between 900 and 750 m a.s.l., which is expressed by a concave upward hypsometric curve with high hypsometric integrals of HI = 0.57 and HI = 0.59 (Fig. 4).

The Vltava and its tributaries show also spatial but less distinct trends in their hypsometry (Fig. 5). The Vltava catchment upstream of Budweis shows a hypsometric maximum at mid-altitude (~ 750 m a.s.l.) and a corresponding S-shaped hypsometric curve with a hypsometric integral of 0.40. Tributaries of the western and northern part of the Vltava catchment such as the Vetší Vltavice, Polecnice and Stražný have hypsometric maxima at elevations between 600 and 700 m a.s.l. and similar hypsometric curves but vary in their hypsometric integrals. The catchments Vetší Vltavice and Polecnice both have hypsometric integrals of 0.36 whereas the Stražný catchment features a higher hypsometric integral of 0.49. Although the Malše and the Stropnice catchments have a long common drainage divide, they show distinct differences in their hypsometric properties. The catchment Malše features a concave upward to slightly S-shaped hypsometric curve with a hypsometric integral of 0.42 while the catchment Stropnice shows a convex upward hypsometric curve with a very low hypsometric integral of 0.20. This is in as far not surprising because the Stropnice mainly drains flat areas north of the BM but reaches significant surface elevation at the watershed to the Malše catchment.

4.4 Longitudinal channel profiles

Field observations suggesting a clear elevation dependence of the topographic features are confirmed by a series of quantitative, morphometric analyses. Longitudinal channel profiles of tributaries of the Danube show a strong correlation between elevation or elevation difference to the receiving stream and channel gradients (Fig. 6). Despite increasing catchment size and thus runoff in downstream direction, channel gradients increase sharply about 200 to 300 m above Danube base level. However, beside this altitudinal trend, we observe also significant differences in channel geometry between the western and eastern part of the study region.

A number of rivers in the western part of the study area (Kleine Mühl, Große Mühl, Pesenbach and Rodl) show similar morphological features (Fig. 6a - d). They are all characterized by few kilometers long, steep headwater segment followed by a tens of kilometers long

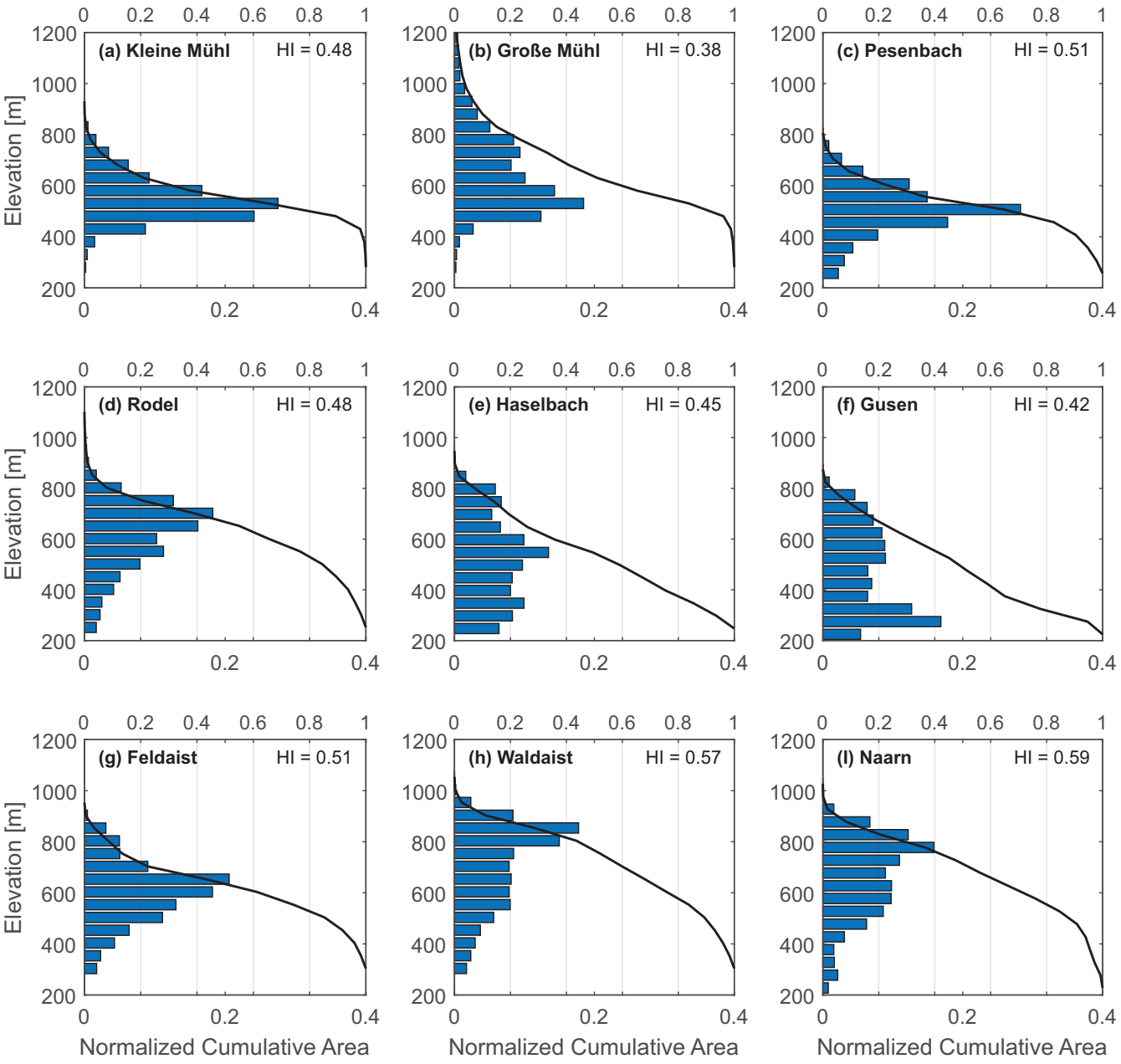

Figure 4: Hypsometric analysis of the Danube tributary catchments. Blue bars indicate the relative fraction of area for each 50 m elevation slice. The black line shows the hypsometric curve. HI is the hypsometric integral.

low gradient segment. These low gradient segments are abruptly terminated by prominent knickpoints roughly at the same elevation level (~ 450 m). Downstream of the knickpoints, channel segments show very high gradients until they finally reach the plain Danube valley, where the channel gradient abruptly decreases. The two westernmost rivers (Fig. 6a, b) lack this segment, as they confluence with the Danube near the "Schlögener Schlingen" where the Danube flows through a deep and narrow gorge without flood plains. Further east, geometric properties of channel length profiles change distinctly. The Haselbach shows a well graded channel profile with a decreasing channel gradient in downstream direction (Fig. 6e). Knickpoints are missing. The further rivers to the east (Gusen, Feldaist, Waldaist, Aist and Naarn) show a shift in the channel geometry from fairly well graded in the west (Gusen) to almost linear in the east (Waldaist) (Fig. 6f - i). All these rivers show a series of knickpoints.

North of the continental divide tributaries of the Vltava reveal similar channel geometries (Fig. 7) than tributaries of the Danube but less clear spatial trends. The channel length profile Vltava-Budweis shows a prominent knickpoint (Fig. 7a). The upper reach of the Vltava forms a well graded channel, which leads into a completely flat section (representing the Lipno reservoir lake) immediately upstream the knickpoint. However, the position of the dam was deliberately chosen in the vicinity of an existing knickpoint, and the two distinct river segments retain their characteristics even if the dam and the artificial lake with a maximum depth of 22 m are removed from

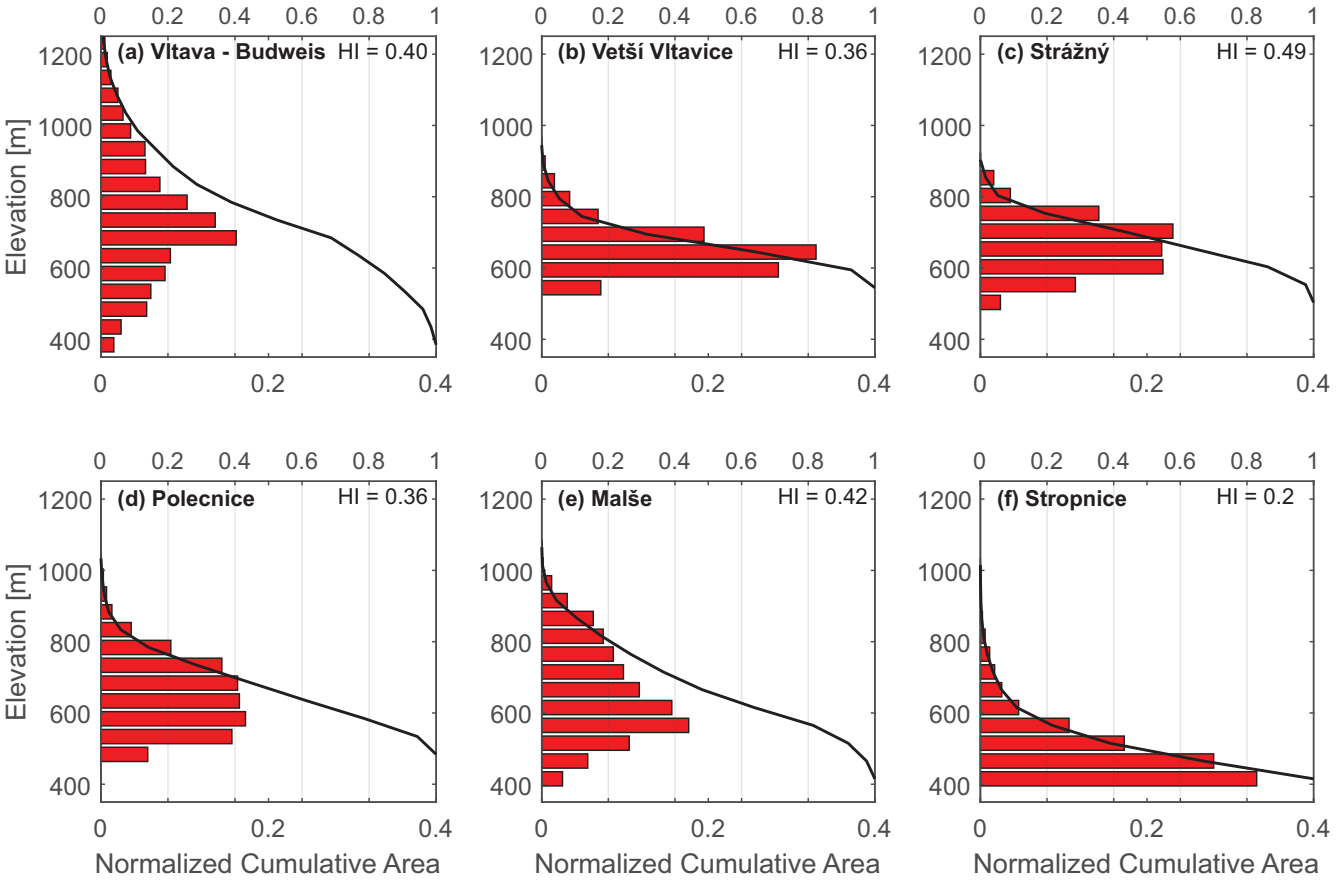

Figure 5: Hypsometric analysis of the Vltava tributary catchments. Red bars indicate the relative fraction of area for each 50 m elevation slice. The black line shows the hypsometric curve. HI is the hypsometric integral.

the analysis (see Fig. 1 for the position of the reservoir). Downstream from the knickpoint a very steep channel segment continues, which eventually transitions into a river segment where the channel gradient remains almost constant for about 80 km despite the fact that the catchment size is doubled from 1000 to 2000 km^2 along this river segment. The channel length profiles of Vetší Vltavice and Všímarský potok both have steep headwaters with a following decrease in channel gradient. The same applies to the river Polecnice, which differ only slightly but its lower lying origin and a series of small steps along its profile. The eastern region of the Vltava catchment is drained by the river Malše and its tributary Stropnice. Along the Malše few knickpoints are observed. The two most prominent knickpoints are located in its upper reach and near the confluence with the Vltava River. Its tributary, the Stropnice, also reveals a distinctive knickpoint separating a segment with very steep headwaters from a segment with a low and roughly constant channel gradient.

4.5 Knickpoints

Large knickpoints in longitudinal river profiles, where the characteristics of the channel and the valley flanks change abruptly, are found both on the Danube and on the Vltava side of the continental divide (Fig. 8). South of the continental divide (Danube drainage system), knickpoints occur over a wide elevations range between ~ 400 m a.s.l. and ~ 850 m a.s.l. and in almost every investigated catchment. However, a distinct cluster of knickpoints at approximately 450 m a.s.l. is observed at the westernmost Danube tributaries of the study area (Kleine Mühl, Große Mühl, Pesenbach and Rodl). While catchments further to the east do not show such a strong break in channel slope at this elevation an increase of mean knickpoint elevation towards east is observed, and hence in downstream direction the Danube as common base level (Fig. 6). The highest knickpoints are found at the easternmost catchments and are located at 850 m a.s.l. (Feldaist) and 840 m a.s.l. (Waldaist). North of the continental divide (Vltava drainage system) knickpoints are located slightly higher compared to those of the Danube drainage system (Figs. 7, 8). They occur at elevations of around 700 m a.s.l. (Vltava-Budweis KP1, Vltava-Budweis KP2, Maltsch KP2). Interestingly, the northeasternmost catchments (Maltsch and Stropnice) show comparable knickpoint elevations such as the rivers south of it (Feldaist, Waldaist and Naarn).

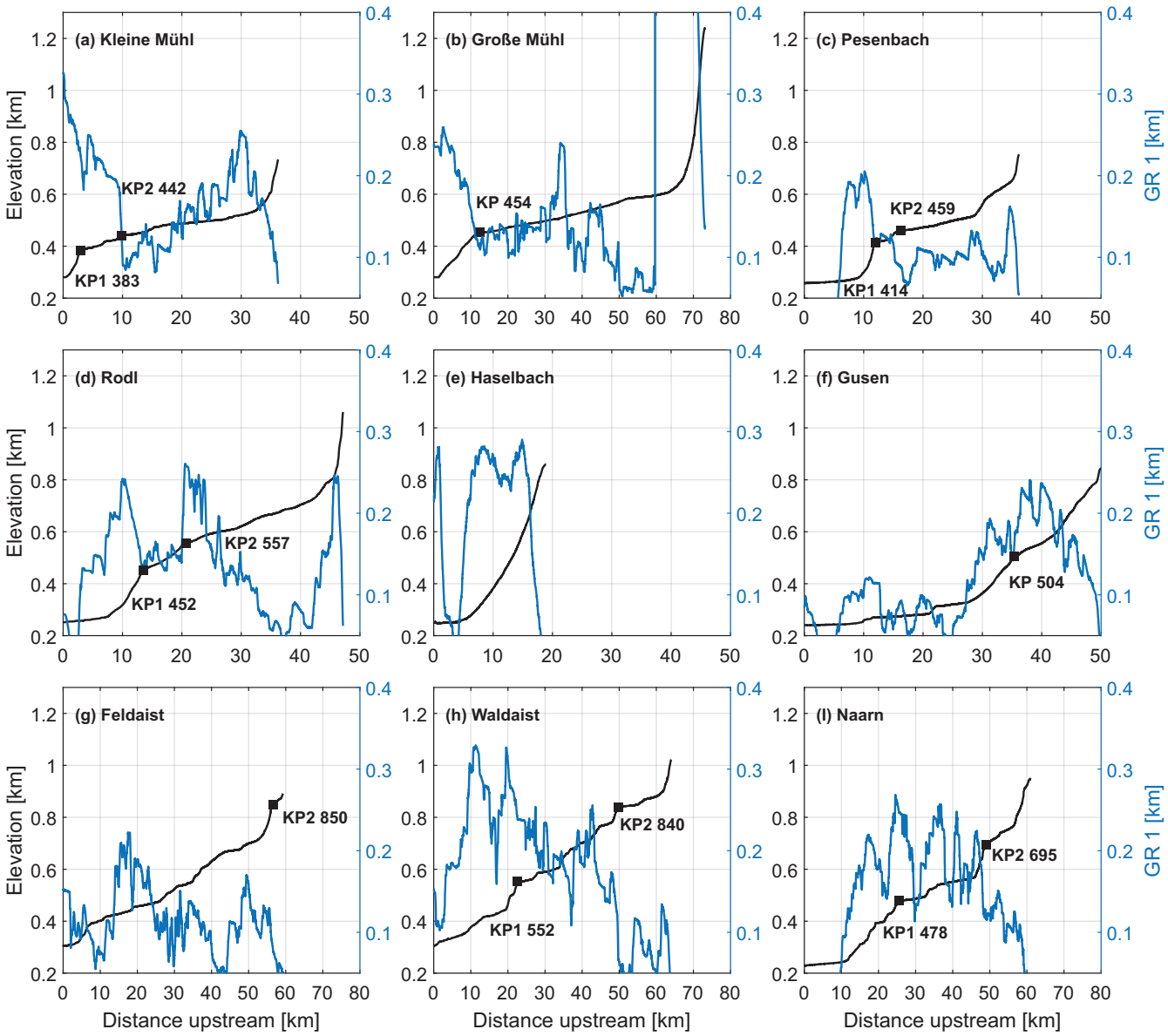

Figure 6: Upstream channel profiles (black lines) and geophysical relief along the channel profiles (blue lines) of selected catchments of the Danube drainage system. Major knickpoints ("KP", black squares) are shown and their elevation is labelled. See Fig. 1 for their spatial position.

4.6 Hypsometric analysis and knickpoints

Comparing the hypsometric analysis with the elevation of knickpoints (Fig. 4), the catchments of the rivers Kleine Mühl, Große Mühl, Pesenbach and Rodl feature a clear trend. Their area-elevation distributions show an abrupt increase of area at elevations above their lowest lying knickpoints. Below, the hypsometric analysis show a rapid decrease in area before entering the Danube. For the other catchments, this trend is less clear. However, for some knickpoints an altitudinal link between a hypsometric maximum and the location of a knickpoint occurs. For example, in the Waldaist catchment, the hypsometric maximum is well in line with the elevation of knickpoint KP2 (840 m a.s.l.). The catchment of river Naarn shows similar hypsometric properties such as the adjacent Waldaist catchment but features noticeable differences in knickpoint elevation. North of the main drainage divide, the biggest catchment Vltava-Budweis features an abrupt increase of area (Fig. 5) at elevations around the knickpoints (KP1 Vltava-Budweis 667 m a.s.l. and KP2 Vltava-Budweis 724 m a.s.l.). Within this catchment the smaller catchments Strážný and Polecnice show at these elevations a rapid decrease of area. For the easternmost catchments of the rivers Malše and Stropnice a link between the hypsometric properties and the location of knickpoints is difficult to make. In the case of the catchment Stropnice the knickpoint KP Stropnice lies within a gradually decreasing area-elevation distribution in upstream direction. A similar situation is observed in the Maltsch catchment where the knickpoints KP1 and KP2 are located at elevations where no visible change in the area-elevation distribution is found.

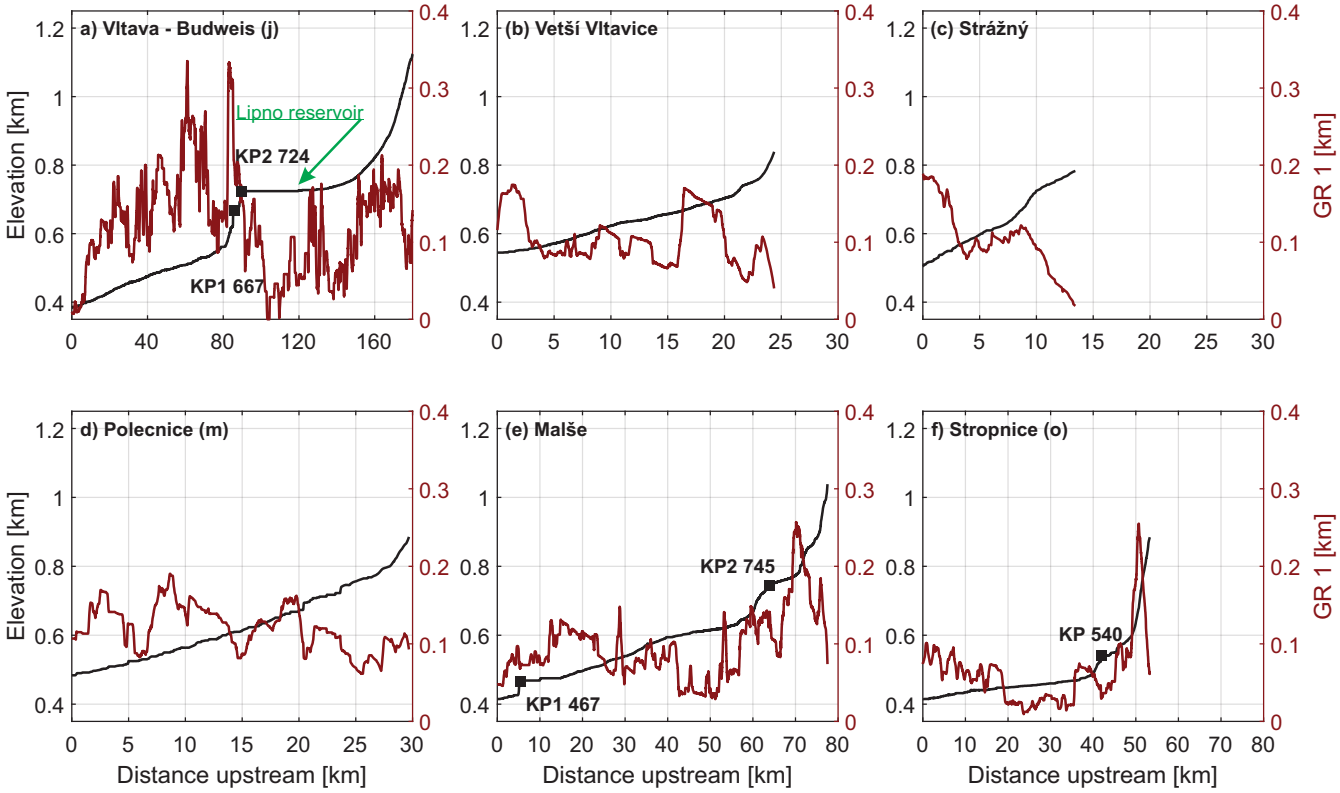

Figure 7: Upstream channel profiles (black lines) and geophysical relief along the channel profiles (red lines) of selected catchments of the Vltava drainage system. Major knickpoints (black squares) are shown and their elevation is annotated. Please see Fig. 1 for their spatial position.

4.7 Geophysical relief

Geophysical relief along channel profiles allows quantifying the field observation that channel segments downstream of major knickpoints are steeper, narrower and bordered by much steeper hillslopes than upstream (Figs. 3, 6, 7). By combining longitudinal river profiles and geophysical relief we now link channel and hillslope properties to decipher the co-evolution of the drainage and hillslope system in the BM. In particular, the westernmost tributaries of the Danube (Fig. 6a-d) show an impressive link between knickpoint position, channel steepness and geophysical relief. These catchments (i.e. Kleine Mühl, Große Mühl, Pesenbach and Rodl) feature high geophysical relief values up to 300 m close to the confluence with the Danube where the channels are steep. The geophysical relief values decrease towards the knickpoints. Lowest geophysical relief values are observed along the channel segments immediately upstream the knickpoints. Catchments in the east (i.e. Gusen, Feldaist, Waldaist and Naarn) show similarities in both their stream profiles and their geophysical relief along the course of the rivers. Starting at their outlets and going upstream, geophysical relief increases to values of about 300 m at mid-altitudes, and decrease rapidly towards the headwaters. The Haselbach with its well graded channel profile, located between the western and eastern group of catchments, shows fairly high (~ 300 m) and rather uniform geophysical relief values along its course. Only close to its confluence with the Danube, where the valley width exceeds the size of the sliding window to compute the geophysical relief, a sudden drop in geophysical relief is observed.

North of the continental divide, in the upper reach of the Vltava River, we observe the same relationship between knickpoint position, channel steepness and geophysical relief (Fig. 7a). The major knickpoints separate the profile in a segment of high geophysical relief values (up to approximately 350 m) downstream and in a segment of noticeably lower geophysical relief values upstream. The small tributaries draining the western and northwestern Vltava catchment (Fig. 7b-d) show a decrease in geophysical relief from their confluence towards their origin. The easternmost catchments Stropnice and Malše have similar geophysical relief profiles. They are characterized by high values at the headwaters (both reach a maximum of 250 m) and a steady decrease downstream followed by a slight increase towards their confluence.

4.8 Normalized steepness index

The previous analyses have characterized the geometry of individual rivers and adjacent hillslopes. Consistent with results from these analyses, figure 9 shows the spatial distribution of steepness index (k_{sn}) in channels. The westernmost tributaries of the Danube (Kleine Mühl, Große Mühl, Pesenbach and Rodl) confluence with the Danube where it incises into the basement rocks of the BM and forms a deep gorge. There, the tributaries show

very high k_{sn} values close to their confluence with the Danube and distinctly lower values upstream of major knickpoints in their channel profiles. However, close to their drainage divides, and in particular north of the divide-parallel valley of the Große Mühl, k_{sn} values increase again. A similar succession of segments with high, low and high k_{sn} values is also observed north of the continental divide in the Vltava catchment. East of the city of Linz, tributaries of the Danube feature very low k_{sn} at elevations close to the base level and higher k_{sn} at mid-elevation river segments. As the upper reaches show distinctly lower k_{sn} values, channel segments of different steepness are separated by knickpoints at mid-elevations.

4.9 χ mapping

Differences in channel steepness between tributaries of the Danube and the Vltava catchment are also indicated by the χ pattern (Fig. 10). Across-divide differences in χ between streams of the two catchments are high along the entire drainage divide. Tributaries of the Danube feature distinctly lower χ values than those of the Vltava River on the directly opposing sides of the drainage divide. Lower χ is tantamount to a higher channel steepness index averaged from the same base level to the origin of the stream at a common drainage divide. The greatest across-divide differences in χ occur at the western (e.g. Große Mühl) and eastern most rivers (e.g. Naarn) of the study area and at a low base level (150 m a.s.l.), where large parts of the respective catchments are considered computing χ (Fig. 10 a). However, across divide gradients in χ become smaller but mainly persist, even by defining a very high base level (400 m a.s.l.) for computing χ (Fig. 10 b). Then only parts of the respective tributary catchments are considered. Gradients vanish only in the central part of the study region (e.g. Rodl). The decrease of across divide gradients in χ with increasing base level indicates that in particular the lower reaches of Danube tributaries feature a higher channel steepness compared to those of the Vltava.

4.10 Slope-elevation distributions

Slope-elevation distributions of the BM were computed for four different domains based on previous analysis indicating a topographic west-east transition within the study area (Fig. 11). These domains represent the western and the eastern part of the Danube and the Vltava catchment, respectively.

The slope-elevation distribution of the western domain of the Danube catchment features a turning point at about 450 to 500 m a.s.l. whereas the eastern domain features a turning point at higher elevations of about 800 to 900 m a.s.l. (Fig. 11 b, c). Turning points of both domains are followed by a significant decrease of slope towards higher elevations. The turning point of the western domain coincides with the average elevation of the knickpoint cluster occurring in this region. The two contrasting slope-elevation distributions of the Danube catchment coincide with other morphological differences (e.g. channel length profiles) between the western and eastern part of the study region. The slope-elevation distribution of the Vltava catchment features less distinct turning points and distinctly lower mean slopes compared to the Danube tributaries (Fig. 11d-f). In particular at lower elevations, mean slopes are up to three times higher at the Danube tributaries than at those of the Vltava. Above the prominent turning point in the slope distributions of the western and eastern Danube tributaries, respectively, mean slopes are similar in catchments on both sides of the drainage divide.

5. Discussion

Observations and a morphometric analysis of the present drainage and hillslope system in the southern BM indicate strong geomorphic disequilibrium that can best be interpreted in terms of progressive landscape rejuvenation. It is reflected in landscape bimodality, where deeply incised valleys at lower elevations contrast low relief landscapes at higher elevations. The spatial distribution of these two different landscape types, which occur in direct vicinity but reflect different stages of landscape evolution, is constrained by the position of knickpoints separating channel segments of different steepness (Fig. 9), hypsometric maxima at mid to high elevations (Figs. 4 and 5) and maxima in geophysical relief at low elevations (Figs. 6 and 7). The transition from steep to low gradient landscapes is consistent with the vertical position of slope maxima in the slope-elevation distributions, which roughly coincide with the knickpoint cluster around 400 – 500 m a.s.l. (Fig. 8). In our study area we found that the observed strong variations in channel steepness and hence the position of major knickpoints is generally unrelated to lithological contacts and the position of faults traces (Fig. 2). However, in the following we develop scenarios that are consistent with the topographic features of the landscape where both temporal and spatial variations in bedrock properties and faults governing the timing and rate of uplift exert first order controls on landscape evolution. Irrespective of these scenarios, we interpret the low-lying high relief areas below the knickpoints as the modern landscape in equilibrium with the current uplift rate, base level, and substrate properties and suggest that the high-lying low relief areas reflect a relic landscape.

5.1 Migration of Danube-Vltava drainage divide

The observed adjustment of landscape geometry is accompanied by the reorganization of river networks and may eventually control the position of the continental drainage divide. For predicting the potential direction of divide migration χ mapping has been employed (Willett et al., 2014; Robl et al., 2017a; Robl et al., 2017b; Forte and Whipple, 2018; Trost et al., 2020). The results indicate

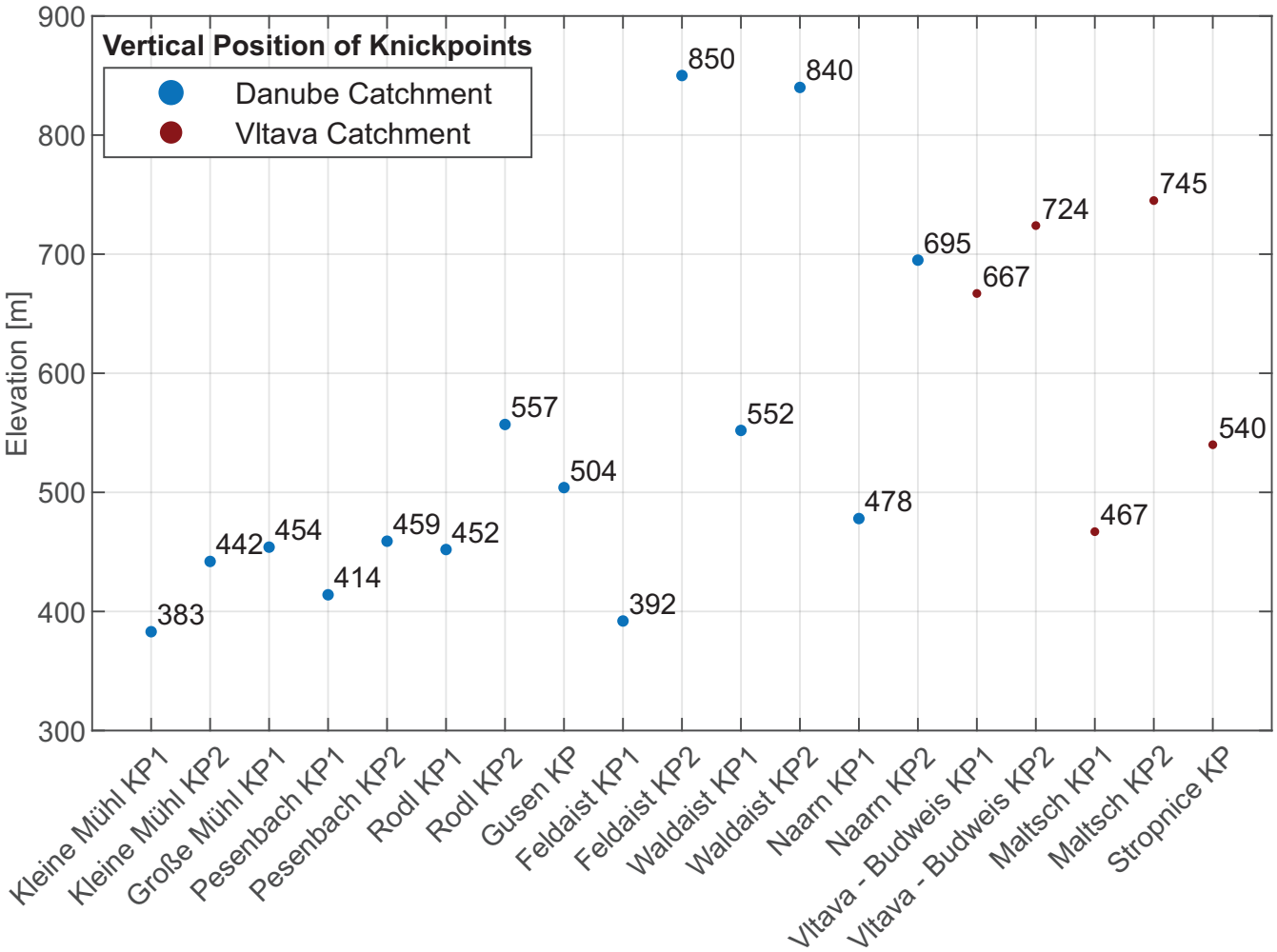

Figure 8: Major knickpoints in channel profiles of Danube (blue dots) and Vltava (red dots) tributaries. The elevation of the knickpoints is labelled. See Fig. 1 for their position in plan view.

a strong drainage divide asymmetry with a steep side (lower χ values) at the Danube and a less steep side at the Vltava (higher χ values) domain. While divide asymmetry is observed at different base levels, the comparison of figures 10a and 10b clearly indicates that the main contribution to the asymmetry originates from the steep lower reaches of the Danube tributaries. Assuming uniform conditions (e.g. substrate properties, uplift rate, climate) steep channels correspond to higher erosion rates and in turn drive the migration of the divide towards the less steep side. Divide migration does not begin until the knickpoints separating steep from less steep channel segments have reached the drainage divide (Robl et al., 2017b; Fan et al., 2021). However, the assumption of uniform conditions has to be justified. The southern BM is built up by different major tectonic units of the Variscan orogen (Fig. 2) which, however, entirely consist of high-grade metamorphic rocks (i.e. gneisses, granulites) and granitic intrusives. It is therefore unlikely that the strong across divide differences in χ are related to contrasting bedrock properties as all these rock types are characterized by a high resistance against erosion. We therefore interpret across divide gradients in χ as an indication for drainage divide mobility. in this case, the Danube will expand its catchment size on expense of those of the Vltava. According to this interpretation, the continental divide will progressively migrate towards north once the knickpoints have reached the drainage divide.

We suggest that the reorganization of drainage networks as indicated by χ also takes place within the Danube and Vltava drainage system. Low gradient, divide-parallel river segments on both sides of the continental divide are increasingly shortened by headward eroding steep north-south (Danube) and south-north (Vltava) flowing rivers. This process eventually causes major river piracy events, which are then reflected by characteristic features in the plan view geometry (i.e. sudden changes in flow direction at the capture point) and in the profile geometry (i.e. mobile knickpoints upstream of the capture point) of the rivers (Robl et al., 2008a; Robl et al., 2017a; Trost et al., 2020). In the BM there are several candidates that may have experienced a river capture event, which however, would have to be confirmed by field work. This could be the case of the northwest - southeast running upper reach of the Vltava, which parallels the continental divide by tens of kilometers before the river

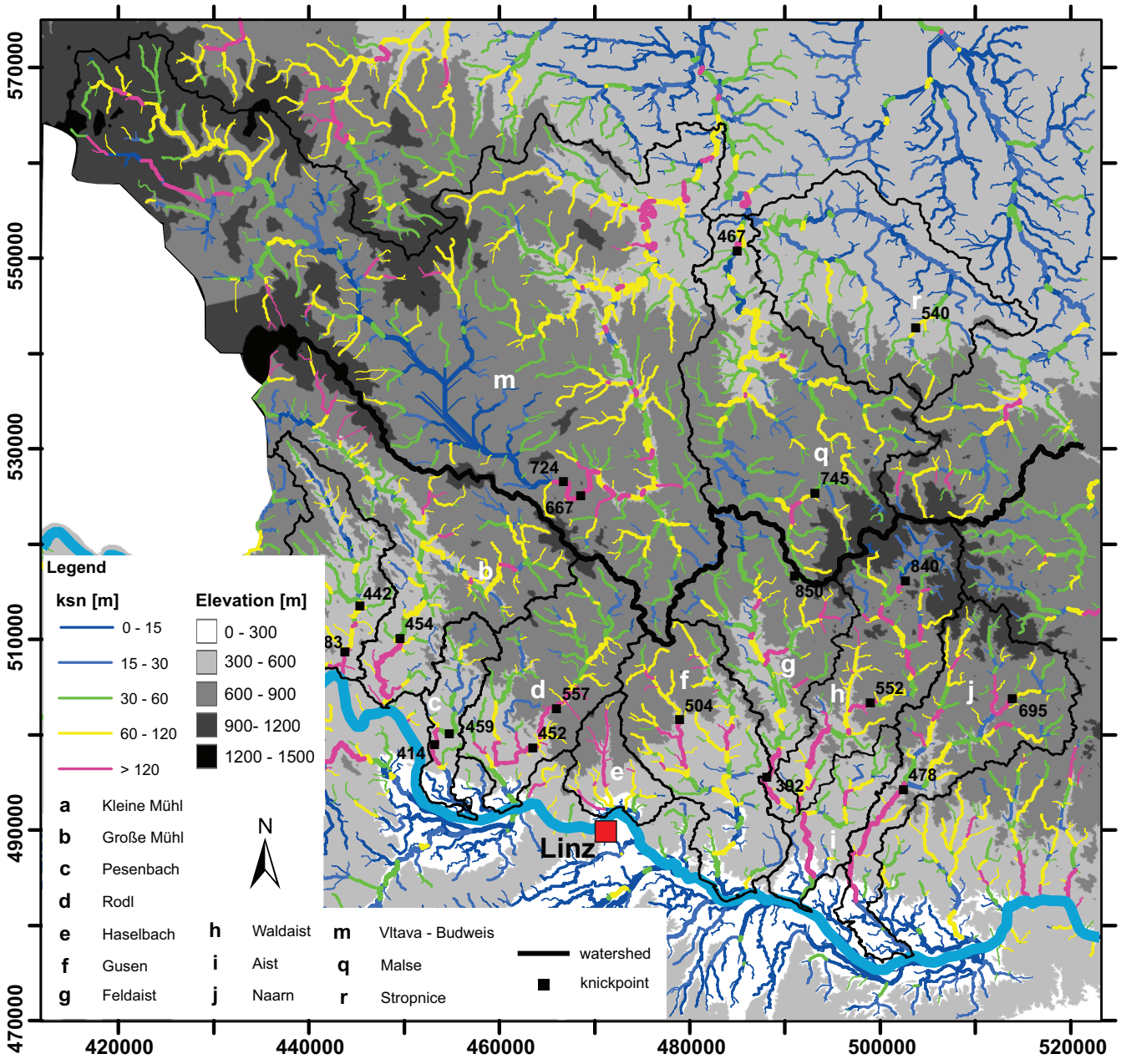

Figure 9: Map of the study area showing the drainage system color-coded for k_{sn}. The continental divide (thick line) and drainage divides (black solid lines) between individual catchments are shown. Major knickpoints (black squares) are plotted and labelled for elevation.

abruptly changes its direction towards the north forming a deeply incised gorge confined towards its upper reach by a mobile knickpoint. Another candidate for such a major river piracy event might be the river Große Mühl with its prominent T-shaped river junction. There, the two largest headwaters of the river Große Mühl follow the same northwest-southeast propagating valley but drain in opposite directions. At the confluence point the river abruptly changes its flow direction towards south. Whether the elbow shaped and T-shaped river section are indicative of river capture events in the BM would need to be substantiated by further investigation (e.g., determination of erosion rates).

5.2 Scenarios of relief rejuvenation

A variety of different drivers have been discussed for landscape bimodality including (a) glacial overprinting of a fluvially conditioned landscape (Brocklehurst and Whipple, 2004; Egholm et al., 2009; Liebl et al., 2021), (b) temporal changes and / or spatial changes in uplift rate (Miller et al., 2013; Robl et al., 2015; Robl et al., 2017b; Liebl et al., 2021) and bedrock properties (Forte et al., 2016; Baumann et al., 2018; Gallen, 2018). In the BM, glacial erosion as a driver can be largely excluded, as the region is outside the major Pleistocene glacial advances with evidence for only a few small glaciers (Nývlt et al., 2011).

Synthesizing findings from our morphological study with the deposition and exhumation history of the

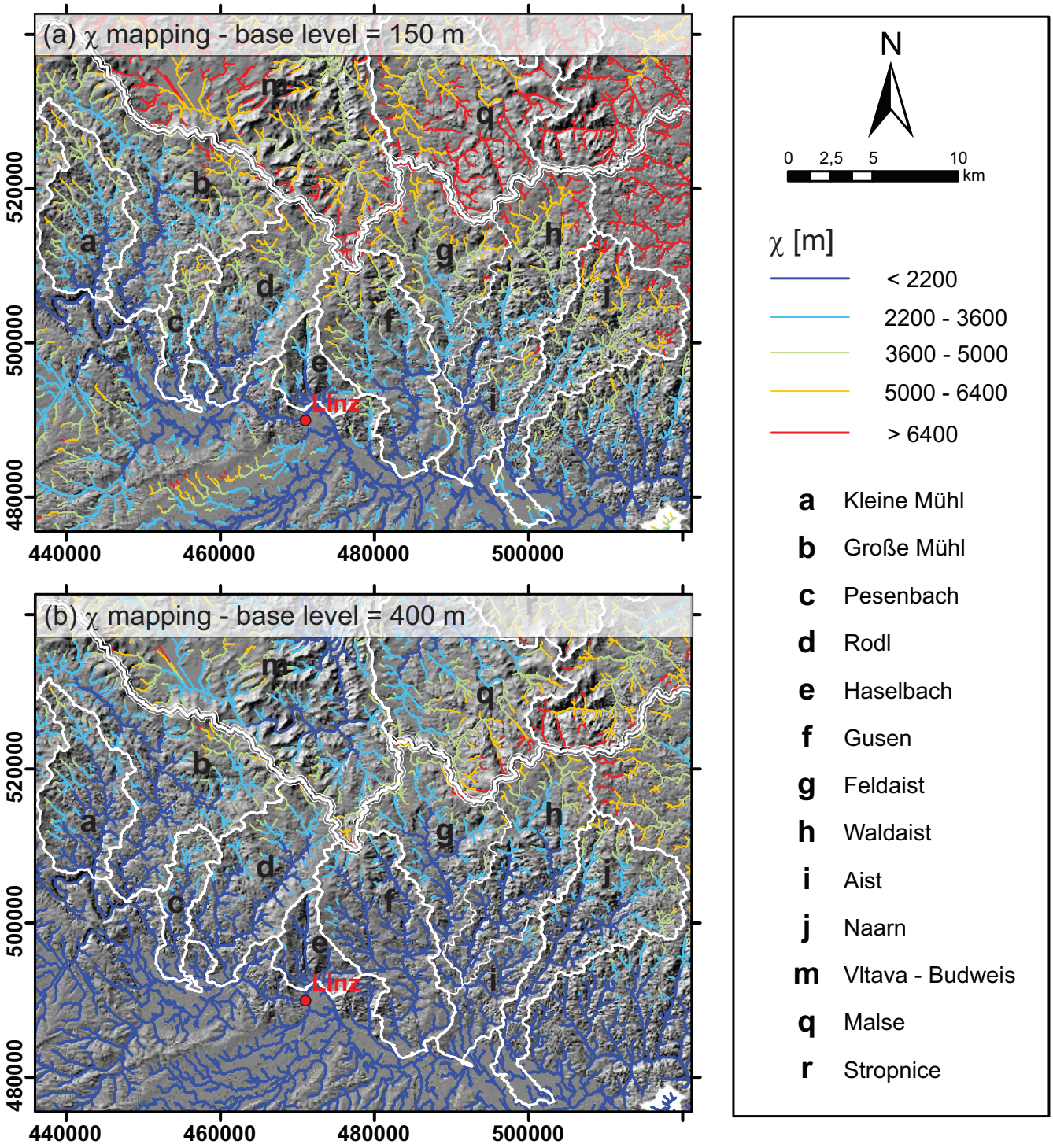

Figure 10: The Danube and Vltava-Labe drainage system color-coded for χ assuming a base level for χ computation of (a) 150 m and (b) 400 m.

nearby Molasse basin (Genser et al., 2007; Gusterhuber et al., 2012; Baran et al., 2014), the most likely interpretation of the observed topographic pattern appears to be a recent regional uplift event (Davis, 1899; Wobus et al., 2006; Hergarten et al., 2010; Robl et al., 2017b). As a characteristic feature, mobile knickpoints evolve in marginal regions and migrate upstream the channels, without corresponding to lithologic contacts or tectonic structures (e.g. Wobus et al., 2006; Robl et al., 2017b). This results in out-of-equilibrium rivers segmented by knickpoints, which lie on the same topographic contour (Fig. 8) (Whipple and Tucker, 1999; Bishop et al., 2005; Wobus et al., 2006). In this scenario, the signal of a large-scale uplift event, which affected major parts of the Eastern Alps and adjacent regions (e.g. Wagner et al., 2010; Baran et al., 2014; Legrain et al., 2015) is progressively transmitted to

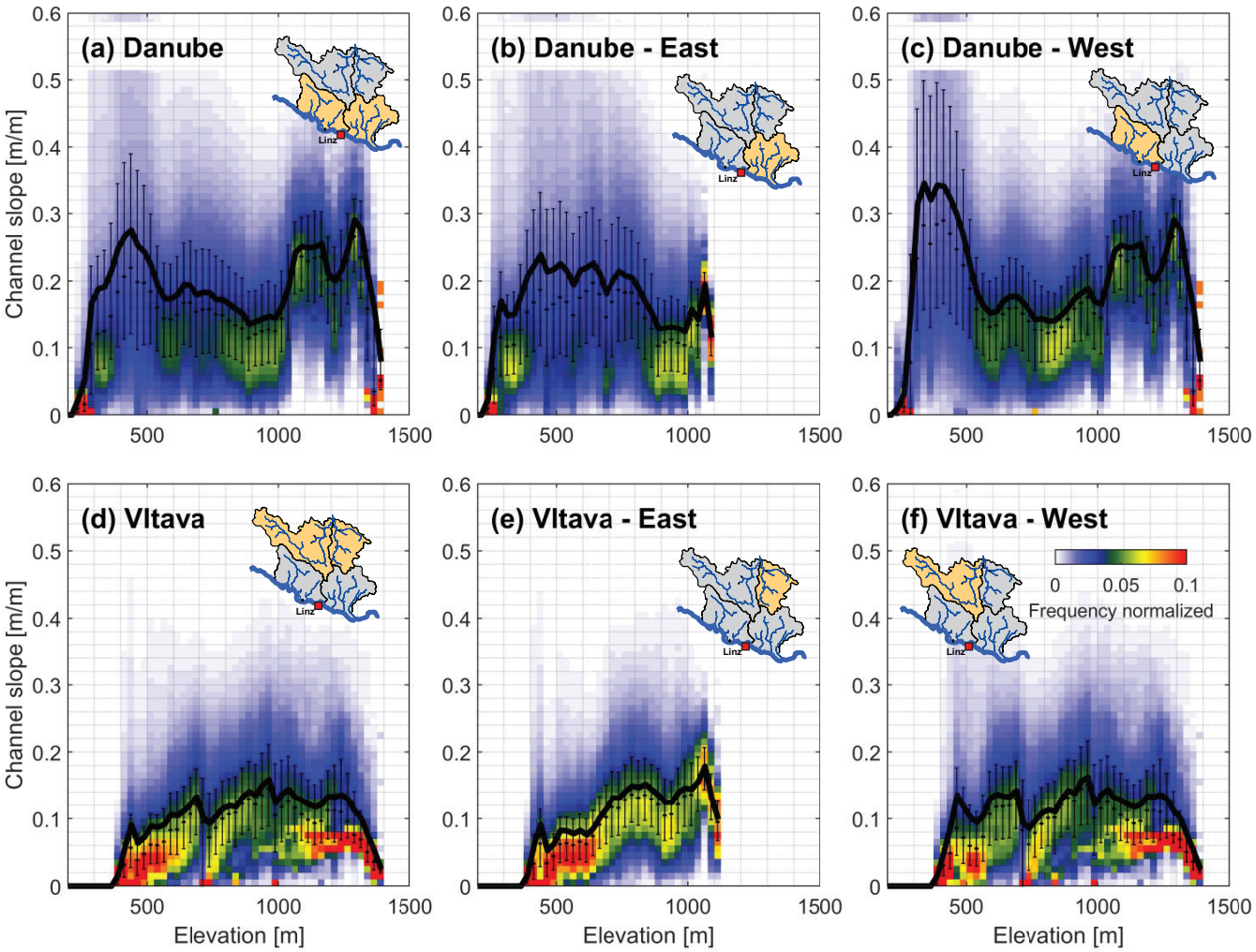

Figure 11: Slope-elevation distributions of the BM. (a) and (d) show the slope-elevation distribution of the main catchments Danube and the Vltava. (b) – (f) show sub domains with catchments predominantly east and west of the Rodl fault and its northern continuation. The inset shows the investigated domain (yellow area).

the BM via the Danube and Vltava rivers and their tributaries. The Danube itself is largely absent of geomorphic disequilibrium features (Robl et al., 2008a) and appears to have been antecedent. This is also testified by the impressive northwards turn of the Danube from its course in the molasse basin towards the elevated topography of the BM in the Strudengau near Dornach and the "Schlögener Schlingen" in the west. These meanders are likely to have been initiated before uplift and retained their shape antecedently through the uplift event. Conversely, the extended low relief landscape some 200 m above the Danube becomes progressively adjusted towards current conditions and allows to predict future changes in the landscape. As a consequence of this relief rejuvenation, steep and low gradient channel segments represent the modern and relic landscape patches, respectively. While many of the morphological properties of the southern Bohemian Massif are consistent with landscape rejuvenation by an uplift event as principal control, the occurrence of several terrain steps and the differences in the elevation of these terrain steps between the western and eastern Danube tributaries cannot be explained by one large-scale uplift event. An explanation for these peculiarities may be found in the fault pattern and the lithological contrast between the Neogene sedimentary cover and the crystalline basement.

Comparisons with the geological map show that the drainage topology is very similar to the present fault system ECRIS (European Cenozoic Rift System) (Ziegler and Dèzes, 2007). It seems that the stream network is adjusting to the evolution of the ECRIS, which is associated with uplift in the Neogene (Ziegler and Dèzes, 2007). While we did not find clear evidence for fault-related changes in the geometry of longitudinal river profiles, the impact of faults on the channel geometry is reported for some regions in the Bohemian Massif (Badura et al., 2007; Popotnig et al., 2013). There, vertical offset at active faults and hence a gradient in the uplift rate field exerts a strong control on the channel steepness in the vicinity of these faults. This, however, does not contradict the idea of a large-scale young uplift event but rather indicates that individual fault-bounded blocks in the Bohemian Massif

rise at different rates. Such a scenario is consistent with the contrasting morphology (i.e. knickpoint position, elevation of hypsometric maxima, slope elevation distribution) of the Danube tributaries west and east of the Rodl fault, which finds its continuation in the Rudolfov-Blanice fault (Vltava catchment), where Popotnig et al. (2013) found strong morphological evidence for recent fault activity.

Bed rock erodibility and its variation in space and time represents a strong control on landscape morphology and channel steepness conditions (e.g. Forte et al., 2016; Baumann et al., 2018; Gallen, 2018; Bernard et al., 2019). Contrast in rock erodibility can lead to completely different topographic features despite uniform climatic and tectonic forcing (e.g. Forte et al., 2016; e.g. Baumann et al., 2018; Gallen, 2018; Bernard et al., 2019). As the crystalline basement of the Bohemian Massif dips southward beneath the sediments of the Molasse Basin, the easily erodible cover rocks lie adjacent to, but also above, the erosion-resistant rocks of the crystalline basement. A similar situation occurs also north of the continental divide in the Vltava catchment. We suggest that the Molasse Basin and the BM where uplifted jointly but that the observed morphological differences between the BM and the adjacent Molasse Basin are controlled by contrasting bedrock properties. The higher channel slopes and eventually higher relief in the BM compared to those of the Molasse Basin is in this scenario associated with the higher resistance of the crystalline bedrock to erosion.

The transition from easily erodible sediments of the Molasse Basin to much less erodible rocks of crystalline basement and the associated emergence of differently steep landscapes involves not only a spatial but also a temporal component. Continuous surface uplift in combination with a sediment pile becoming thicker towards the south, causes rivers, such as the Danube, to incise to the point where the crystalline basement is reached. Because of the lower erodibility of these rocks, the channel gradients existing at that time (yet in equilibrium with the more easily erodible rocks of the Molasse Basin) are not sufficient to balance the rate of uplift by the rate of erosion. As long as the profile geometry of these rivers is not adjusted to the new substrate properties by channel steepening, they will be uplifted. In this scenario, such rivers are becoming increasingly prone to be captured by rivers further south still flowing in easily erodible Molasse sediments and thus at a lower elevation. Such a scenario could nicely explain the shift of the Danube River towards south. The succeeding rapid baselevel fall can consistently explain the emergence of a stepped landscape during continuous long-lasting uplift at low rates. Such a scenario does not involve large gradients in the uplift rate nor the occurrence of multiple enigmatic uplift pulses within the study region, but the transmission of the uplift signal via major rivers (i.e. Danube, Vltava) from the far field. The strong lithological contrasts suffice creating the varying topographic expressions between regions covered by Neogene sediments and crystalline basement and can also lead to transient river profiles with steep lower and less steep upper reaches as observed in the western Danube tributaries.

The timing of the inferred young uplift of several hundred vertical meters in the southern BM is not very well constrained, but it is clearly younger than the time scale of fluvially driven geomorphic equilibration. It is thus likely to be of the order of a few million years. Attempts to decipher the role of uplift in the region of the BM have been made by recent studies (Ziegler and Dèzes, 2007; Gusterhuber et al., 2012; Baran et al., 2014) discussing lithospheric processes as the driving forces behind uplift. However, an uplift event in the last few million years regardless of the cause can consistently explain the present topographic characteristics.

The coexistence of different influences that affect channel steepness and relief morphology in similar ways can lead to ambiguity about the origin of morphological features (Wobus et al., 2006; Robl et al., 2015; Liebl et al., 2021). While the impact of glaciers can be ruled out, neither control in the latter two cases (i.e. gradients in the uplift rates, contrasting substrate properties) can typically be dismissed or be used as the only explanation on the basis of a morphometric analysis. The scenarios described show that an interplay of large-scale uplift, local fault activity, and contrasting bedrock properties caused most likely the morphological peculiarities of the BM. To reveal the respective contributions of these controls and to decipher the recent erosion history requires in addition to the morphometric analysis a comprehensive field study based on neotectonics and on cosmogenic nuclides (^{10}Be and ^{26}Al) of river sediments.

6. Conclusions

In this study we investigated landscape properties of the BM to constrain the latest topographic evolution. Based on morphological analyses in combination with observations we come to the following conclusions:

In the BM, there is strong evidence for landscape bimodality. It is expressed in the co-existence of modern and relic landscapes, which exhibit different morphologies. Low-lying modern landscapes feature high relief surfaces with deeply incised gorges whereas relic landscapes at higher elevations are characterized by low relief surfaces with wide valleys and planation surfaces.

- The occurrence of knickpoint clusters in the BM do not correspond to lithological contacts or tectonic structures. The knickpoints are located at similar elevations, and we attribute these knickpoints to either temporal changes in uplift rate or a baselevel lowering due to a major river piracy event or a combination of both.
- Across divide gradients in χ, with steeper channels at the Danube side on average indicate a northward migration of the Danube-Vltava drainage divide. Consequently, the Danube catchment grows on expense

of the Vltava catchment, which eventually causes major river piracy events.
- We attribute the mountainous landscape and relief rejuvenation of the BM to uplift of several hundred vertical meters on a time scale that is short compared to the time scale of fluvial equilibration.
- We suggest that the occurrence of contrasting bedrock properties between Molasse sediments and the crystalline basement represents a superior control on the topographic evolution of the entire region. The transition from soft sediments of the Molasse basin to much less erodible basement rocks during progressive river incision in a setting of low but long lasting uplift distinctly changes the channel steepness and relief, the course of the receiving streams, and their susceptibility to sudden changes in flow direction (river capture).

Acknowledgements

This study was supported by the Austrian Science Fund (FWF) and the government of Salzburg through the project ELEvATE: Elevated Low Relief Landscapes in Mountain Belts (P 31609). We thank Kryštof Verner for providing the 10 m DEM of the Czech Republic (Copyright © 2010 CÚZK, all rights reserved). We thank Hugo Ortner for the editorial handling and the two reviewers Joel Leonhard and Kurt Decker for their detailed comments and constructive suggestions to improve the manuscript.

References

Badura J., Zuchiewicz W., Štěpančiková P., Przybylski B., Kontny B., Cacoń, S., 2007. The sudetic marginal fault: A young morphophotectonic feature at the NE margin of the Bohemian Massif, Central Europe. Acta Geodynamica et Geomaterialia, 4/4, 7–29

Balatka B., Kalvoda J., 2008. Evolution of Quaternary river terraces related to the uplift of the central part of the Bohemian Massif. Geografie. Sbornik Ceské geografické spolecnosti, 113/3, 205–222

Baran R., Friedrich A.M., Schlunegger F., 2014. The late Miocene to Holocene erosion pattern of the Alpine foreland basin reflects Eurasian slab unloading beneath the western Alps rather than global climate change. Lithosphere, 6/2, 124–131. https://doi.org/10.1130/L307.1

Baumann S., Robl J., Prasicek G., Salcher B., Keil M., 2018. The effects of lithology and base level on topography in the northern alpine foreland. Geomorphology, 313, 13–26. https://doi.org/10.1016/j.geomorph.2018.04.006

Bernard T., Sinclair H.D., Gailleton B., Mudd S.M., Ford M., 2019. Lithological control on the post-orogenic topography and erosion history of the Pyrenees. Earth and Planetary Science Letters, 518, 53–66. https://doi.org/10.1016/j.epsl.2019.04.034

Bishop P., Hoey T. B., Jansen J D., Artza I.L., 2005. Knickpoint recession rate and catchment area: the case of uplifted rivers in Eastern Scotland. Earth Surface Processes and Landforms: The Journal of the British Geomorphological Research Group, 30/6, 767–778. https://doi.org/10.1002/esp.1191

Bourgeois O., Ford M., Diraison M., Veslud C., Gerbault M., Pik R., Ruby N., Bonnet S., 2007. Separation of rifting and lithospheric folding signatures in the NW-Alpine foreland. International Journal of Earth Sciences, 96/6, 1003–1031. 10.1007/s00531-007-0202-2

Brandmayr M., Loizenbauer J., Wallbrecher E., 1999. Contrasting PT conditions during conjugate shear zone development in the Southern Bohemian Massif, Austria. Mitteilungen der Österreichischen Geologischen Gesellschaft, 90, 11–29

Brocklehurs, S.H., Whipple K.X., 2004. Hypsometry of glaciated landscapes. Earth Surface Processes and Landforms, 29/7, 907–926. https://doi.org/10.1002/esp.1083

Cháb J., Stráník Z., Eliáš M., 2007. Geologická mapa České republiky 1: 500 000, Česká geologická služba.

Champagnac J., Molnar P., Anderson R., Sue C., Delacou B., 2007. Quaternary erosion-induced isostatic rebound in the western Alps. Geology, 35/3, 195–198. https://doi.org/10.1130/G23053A.1

Cheng K.-Y., Hung J.-H., Chang H.-C., Tsai H., Sung Q.-C., 2012. Scale independence of basin hypsometry and steady state topography. Geomorphology, 171, 1–11. https://doi.org/10.1016/j.geomorph.2012.04.022

Danišík M., Migoń P., Kuhlemann J., Evans N. J., Dunkl I., Frisch, W., 2010. Thermochronological constraints on the long-term erosional history of the Karkonosze Mts., Central Europe. Geomorphology, 117/1-2, 78–89. https://doi.org/10.1016/j.geomorph.2009.11.010

Davis W.M., 1899. The geographical cycle. The Geographical Journal, 14/5, 481–504

Dethier D.P., Ouimet W., Bierman P.R., Rood D.H., Balco G., 2014. Basins and bedrock: Spatial variation in 10Be erosion rates and increasing relief in the southern Rocky Mountains, USA. Geology, 42/2, 167-170. https://doi.org/10.1130/G34922.1

Egger H., Krenmayr H., Mandl G., Matura A., Nowotny A., Pascher G., Pestal G., Pistotnik J., Rockenschaub M., Schnabel W., 1999. Geologische Übersichtskarte der Republik Österreich 1: 1500000. Geologische Bundesanstalt, Wien.

Egholm D., Nielsen S., Pedersen V., Lesemann J.-E., 2009. Glacial effects limiting mountain height. Nature, 460/7257, 884–887. https://doi.org/10.1038/nature08263

England P., Houseman G., 1986. Finite strain calculations of continental deformation: 2. Comparison with the India-Asia collision zone. Journal of Geophysical Research: Solid Earth, 91/B3, 3664–3676. https://doi.org/10.1029/JB091iB03p03664

Fan N., Kong P., Robl J.C., Zhou H., Wang X., Jin Z., Liu X., 2021. Timing of river capture in major Yangtze River tributaries: Insights from sediment provenance and morphometric indices. Geomorphology, 392, 107915. https://doi.org/10.1016/j.geomorph.2021.107915

Finger F., Gerdes A., Janousek V., Rene M., Riegler G., 2007. Resolving the Variscan evolution of the Moldanubian sector of the Bohemian Massif: the significance of the Bavarian and the Moravo-Moldanubian tectonometamorphic phases. Journal of Geosciences, 52/1–2, 9–28. http://doi.org/10.3190/jgeosci.005

Finger F., Gerdes A., Rene M., Riegler G., 2009. The Saxo-Danubian Granite Belt: magmatic response to post-collisional delamination of mantle lithosphere below the southwestern sector of the Bohemian Massif (Variscan orogen). Geologica Carpathica, 60/3, 205. https://doi.org/10.2478/v10096-009-0014-3

Flint J.-J., 1974. Stream gradient as a function of order, magnitude, and discharge. Water Resources Research, 10/5, 969–973. https://doi.org/10.1029/WR010i005p00969

Forte A. M., Whipple K.X., 2018. Criteria and tools for determining drainage divide stability. Earth and Planetary Science Letters, 493, 102–117. https://doi.org/10.1016/j.epsl.2018.04.026

Forte A.M., Yanites B.J., Whipple K.X., 2016. Complexities of landscape evolution during incision through layered stratigraphy with contrasts in rock strength. Earth Surface Processes and Landforms, 41/12, 1736–1757. https://doi.org/10.1002/esp.3947

Franke W., 2014. Topography of the Variscan orogen in Europe: failed–not collapsed. International Journal of Earth Sciences, 103/5, 1471–1499. https://doi.org/10.1007/s00531-014-1014-9

Fuchs G., Matura A., 1976. Zur Geologie des Kristallins der südlichen Bohmischen Masse.(Géologie du cristallin dans le Sud du massif de Bohême). Jahrbuch der Geologischen Bundesanstalt Wien, 119/1, 1–45

Gallen S.F., 2018. Lithologic controls on landscape dynamics and aquatic species evolution in post-orogenic mountains. Earth and Planetary Science Letters, 493, 150–160. https://doi.org/10.1016/j.epsl.2018.04.029

Genser J., Cloetingh S.A., Neubauer F., 2007. Late orogenic rebound and oblique Alpine convergence: new constraints from subsidence analysis of the Austrian Molasse basin. Global and Planetary Change, 58/1–4, 214–223. https://doi.org/10.1016/j.gloplacha.2007.03.010

Gusterhuber J., Dunkl I., Hinsch R., Linzer H.-G., Sachsenhofer R., 2012. Neogene uplift and erosion in the Alpine foreland basin (upper Austria and Salzburg). Geologica Carpathica, 63/4, 295. https://doi.org/10.2478/v10096-012-0023-5

Hack J.T., 1957. Studies of longitudinal stream profiles in Virginia and Maryland: US Government Printing Office.

Hantke R., 1993. Flussgeschichte Mitteleuropas: Skizzen zu einer Erd-, Vegetations-, und Klimageschichte der letzten 40 Millionen Jahre, Enke, Stuttgard, 460 pp.

Harel M.A., Mudd S.M., Attal M., 2016. Global analysis of the stream power law parameters based on worldwide 10Be denudation rates. Geomorphology, 268, 184–196. https://doi.org/10.1016/j.geomorph.2016.05.035

Hejl E., Coyle D., Lal N., den Haute P.V., Wagner G.A., 1997. Fission-track dating of the western border of the Bohemian massif: thermochronology and tectonic implications. Geologische Rundschau, 86/1, 210–219. 10.1007/s005310050133

Hejl E., Sekyra G., Friedl G., 2003. Fission-track dating of the south-eastern Bohemian massif (Waldviertel, Austria): thermochronology and long-term erosion. International Journal of Earth Sciences, 92/5, 677–690. https://doi.org/10.1007/s00531-003-0342-y

Hergarten S., Robl J., Stüwe K., 2016. Tectonic geomorphology at small catchment sizes–extensions of the stream-power approach and the χ method. Earth Surface Dynamics, 4/1, 1–9. https://doi.org/10.5194/esurf-4-1-2016

Hergarten S., Wagner T., Stüwe K., 2010. Age and prematurity of the Alps derived from topography. Earth and Planetary Science Letters, 297/3–4, 453–460. https://doi.org/10.1016/j.epsl.2010.06.048

Homolová D., Lomax J., Špaček P., Decker K., 2012. Pleistocene terraces of the Vltava River in the Budějovice basin (Southern Bohemian Massif): New insights into sedimentary history constrained by luminescence data. Geomorphology, 161–162, 58–72. https://doi.org/10.1016/j.geomorph.2012.04.001

Howard A.D., Dietrich W.E., Seidl M.A., 1994. Modeling fluvial erosion on regional to continental scales. Journal of Geophysical Research: Solid Earth, 99/B7, 13971–13986. https://doi.org/10.1029/94JB00744

Kirby E., Whipple K.X., 2012. Expression of active tectonics in erosional landscapes. Journal of Structural Geology, 44, 54–75. https://doi.org/10.1016/j.jsg.2012.07.009

Kossmat F., 1927. Gliederung des varistischen Gebirgsbaues. Abhandlungen Sächsischen Geologischen Landesamts, 1, 1–39.

Kroner U., Romer R.L., 2013. Two plates — Many subduction zones: The Variscan orogeny reconsidered. Gondwana Research, 24/1, 298–329. https://doi.org/10.1016/j.gr.2013.03.001

Kuhlemann J., Dunkl I., Brügel A., Spiegel C., Frisch W., 2006. From source terrains of the Eastern Alps to the Molasse Basin: Detrital record of non-steady-state exhumation. Tectonophysics, 413/3–4, 301–316. https://doi.org/10.1016/j.tecto.2005.11.007

Kühni A., Pfiffner O.-A., 2001. The relief of the Swiss Alps and adjacent areas and its relation to lithology and structure: topographic analysis from a 250-m DEM. Geomorphology, 41/4, 285–307. https://doi.org/10.1016/S0169-555X(01)00060-5

Lague D., 2014. The stream power river incision model: evidence, theory and beyond. Earth Surface Processes and Landforms, 39/1, 38–61. https://doi.org/10.1002/esp.3462

Lange J.-M., Tonk C., Wagner G. A., 2008. Apatitspaltspurdaten zur postvariszischen thermotektonischen Entwicklung des sächsischen Grundgebirges - erste Ergebnisse. Zeitschrift der deutschen Gesellschaft für Geowissenschaften/159, 122–132.

Legrain N., Dixon J., Stüwe K., von Blanckenburg F., Kubik P., 2015. Post-Miocene landscape rejuvenation at the eastern end of the Alps. Lithosphere, 7/1, 3–13. https://doi.org/10.1130/L391.1

Legrain N., Stüwe K., Wölfler A., 2014. Incised relict landscapes in the eastern Alps. Geomorphology, 221, 124–138. https://doi.org/10.1016/j.geomorph.2014.06.010

Lenhardt W.A., Švancara J., Melichar P., Pazdírkov, J., Havíř J., Sýkorová Z., 2007. Seismic activity of the Alpine-Carpathian-Bohemian Massif region with regard to geological and potential field data. Geologica Carpathica, 58/4, 397–412.

Liebl M., Robl J., Egholm D.L., Prasicek G., Stüwe K., Gradwohl G., Hergarten S., 2021. Topographic signatures of progressive glacial landscape transformation. Earth Surface Processes and Landforms, 46/10, 1964–1980. https://doi.org/10.1002/esp.5139

Linner M., Finger F., Reiter E., 2011. Moldanubikum (Kristallin der Böhmischen Masse). In: Rupp, C., Linner, M., Mandl, G. (eds.), Oberösterreich, Geologie der österreichischen Bundesländer: Wien, Geologische Bundesanstalt, pp. 29–50.

Mackenbach R., 1984. Jungtertiäre Entwässerungsrichtungen zwischen Passau und Hausruck (O.Ö). Köln, Geologisches Institut der Universität Köln, Sonderveröffentlichung, 175 pp

Mandal S.K., Lupker M., Burg, J.-P. Valla P. G., Haghipour N., Christl, M., 2015. Spatial variability of 10Be-derived erosion rates across the southern Peninsular Indian escarpment: A key to landscape evolution across passive margins. Earth and Planetary Science Letters, 425, 154–167. https://doi.org/10.1016/j.epsl.2015.05.050

Miller S.R., Sak P.B., Kirby E., Bierman P.R., 2013. Neogene rejuvenation of central Appalachian topography: Evidence for differential rock uplift from stream profiles and erosion rates. Earth and Planetary Science Letters, 369–370, 1–12. https://doi.org/10.1016/j.epsl.2013.04.007

Nývlt D., Engel Z., Tyráček J., 2011. Pleistocene glaciations of Czechia, Developments in quaternary sciences, Volume 15, Elsevier, pp. 37–46. https://doi.org/10.1016/B978-0-444-53447-7.00004-0

O'Brien P.J., Carswell D. A., 1993. Tectonometamorphic evolution of the Bohemian Massif: evidence from high pressure metamorphic rocks. Geologische Rundschau, 82/3, 531–555. 10.1007/BF00212415

O'Callaghan J.F., Mark D.M., 1984. The extraction of drainage networks from digital elevation data. Computer Vision, Graphics, and Image Processing, 28/3, 323–344. https://doi.org/10.1016/S0734-189X(84)80011-0

Ohmori H., 1993. Changes in the hypsometric curve through mountain building resulting from concurrent tectonics and denudation. Geomorphology, 8/4, 263–277. https://doi.org/10.1016/0169-555X(93)90023-U

Olivetti V., Godard V., Bellier O., 2016. Cenozoic rejuvenation events of Massif Central topography (France): Insights from cosmogenic denudation rates and river profiles. Earth and Planetary Science Letters, 444, 179–191. https://doi.org/10.1016/j.epsl.2016.03.049

Pánek T., Kapustová V., 2016. Long-Term Geomorphological History of the Czech Republic. in Pánek, T., Hradecký, J., eds., Landscapes and Landforms of the Czech Republic: Cham, Springer International Publishing, pp. 29–39. https://doi.org/10.1007/978-3-319-27537-6_4

Perron, J.T., Royden L., 2013. An integral approach to bedrock river profile analysis. Earth Surface Processes and Landforms, 38/6, 570–576. https://doi.org/10.1002/esp.3302

Popotnig A., Tscheg, D., Decker K., 2013. Morphometric analysis of a reactivated Variscan fault in the southern Bohemian Massif (Budějovice basin, Czech Republic). Geomorphology, 197, 108–122. https://doi.org/10.1016/j.geomorph.2013.04.042

Robl J., Heberer B., Prasicek G., Neubauer F., Hergarten S., 2017a. The topography of a continental indenter: The interplay between crustal deformation, erosion, and base level changes in the eastern Southern Alps. Journal of Geophysical Research: Earth Surface, 122/1, 310–334. https://doi.org/10.1002/2016JF003884

Robl J., Hergarten S., Prasicek, G., 2017b. The topographic state of fluvially conditioned mountain ranges. Earth-Science Reviews, 168, 190–217. https://doi.org/10.1016/j.earscirev.2017.03.007

Robl J., Hergarten S., Stüwe K., 2008a. Morphological analysis of the drainage system in the Eastern Alps. Tectonophysics, 460/1, 263–277. https://doi.org/10.1016/j.tecto.2008.08.024

Robl J., Prasicek G., Hergarten S., Stüwe K., 2015. Alpine topography in the light of tectonic uplift and glaciation. Global and Planetary Change, 127, 34–49. https://doi.org/10.1016/j.gloplacha.2015.01.008

Robl J., Stüwe K., 2005a. Continental collision with finite indenter strength: 1. Concept and model formulation. Tectonics, 24/4. https://doi.org/10.1029/2004TC001727

Robl J., Stüwe K., 2005b. Continental collision with finite indenter strength: 2. European Eastern Alps. Tectonics, 24/4. https://doi.org/10.1029/2004TC001741

Robl J., Stüwe K., Hergarten S., 2008b. Channel profiles around Himalayan river anticlines: Constraints on their formation from digital elevation model analysis. Tectonics, 27/3. https://doi.org/10.1029/2007TC002215

Royden L., Taylor Perron J., 2013. Solutions of the stream power equation and application to the evolution of river longitudinal profiles. Journal of Geophysical Research: Earth Surface, 118/2, 497–518. https://doi.org/10.1002/jgrf.20031

Schäfer A., 1989. Variscan molasse in the Saar-Nahe Basin (W-Germany), Upper Carboniferous and Lower Permian. Geologische Rundschau, 78/2, 499–524. https://doi.org/10.1007/BF01776188

Schwanghart W., Kuhn N.J., 2010. TopoToolbox: A set of Matlab functions for topographic analysis. Environmental Modelling & Software, 25/6, 770–781. https://doi.org/10.1016/j.envsoft.2009.12.002

Schwanghart W., Scherler D., 2014. Short Communication: TopoToolbox 2 – MATLAB-based software for topographic analysis and modeling in Earth surface sciences. Earth Surface Dynamics, 2/1, 1–7. https://doi.org/10.5194/esurf-2-1-2014

Schwanghart W., Scherler D., 2017. Bumps in river profiles: uncertainty assessment and smoothing using quantile regression techniques. Earth Surf. Dynam., 5/4, 821–839. 10.5194/esurf-5-821-2017

Small E.E., Anderson R.S., 1998. Pleistocene relief production in Laramide mountain ranges, western United States. Geology, 26/2, 123–126. https://doi.org/10.1130/0091-7613(1998)026<0123:PRPILM>2.3.CO;2

Strahler A.N., 1952. Hypsometric (area-altitude) analysis of erosional topography. Geological Society of America Bulletin, 63/11, 1117-1142. https://doi.org/10.1130/0016-7606(1952)63[1117:HAAOET]2.0.CO;2

Stüwe K., Hohmann K., 2021. The Relic Landscapes of the Grazer Bergland: Revisiting the Piedmonttreppen Debate. Austrian Journal of Earth Sciences, 114/1, 46–65. https://doi.org/10.17738/ajes.2021.0003

Trost G., Robl J., Hergarten S., Neubauer F., 2020. The destiny of orogen-parallel streams in the Eastern Alps: the Salzach–Enns drainage system. Earth Surface Dynamics, 8/1, 69–85. https://doi.org/10.5194/esurf-8-69-2020

Tschegg D., Decker K., 2013. Distinguishing Quaternary and Pre-Quaternary clastic sediments in the vicinity of České Budejovice (Southern Bohemian Massif, Czech Republic). Austrian Journal of Earth Sciences, 106/1, 72–89.

Tyráček J., Havlíček P., 2009. The fluvial record in the Czech Republic: A review in the context of IGCP 518. Global and Planetary Change, 68/4, 311–325. https://doi.org/10.1016/j.gloplacha.2009.03.007

Vamvaka A., Siebel W., Chen F., Rohrmüller J., 2014. Apatite fission-track dating and low-temperature history of the Bavarian Forest (southern Bohemian Massif). International Journal of Earth Sciences, 103/1, 103–119. https://doi.org/10.1007/s00531-013-0945-x

Wagner T., Fabel D., Fiebig M., Häuselmann P., Sahy D., Xu S., Stüwe K., 2010. Young uplift in the non-glaciated parts of the Eastern Alps. Earth and Planetary Science Letters, 295/1, 159–169. https://doi.org/10.1016/j.epsl.2010.03.034

Wagner T., Fritz H., Stüwe K., Nestroy O., Rodnight H., Hellstrom J., Benischke R., 2011. Correlations of cave levels, stream terraces and planation surfaces along the River Mur—Timing of landscape evolution along the eastern margin of the Alps. Geomorphology, 134/1, 62–78. https://doi.org/10.1016/j.geomorph.2011.04.024

Wessely G., 2006. Geologie der österreichischen Bundesländer: Niederösterreich. Geologische Bundesanstalt, Wien, 416 pp.

Whipple K.X., 2004. Bedrock rivers and the geomorphology of active orogens. Annual Review of Earth and Planetary Sciences, 32/1, 151–185. https://doi.org/10.1146/annurev.earth.32.101802.120356

Whipple K.X., Tucker G.E., 1999. Dynamics of the stream-power river incision model: Implications for height limits of mountain ranges, landscape response timescales, and research needs. Journal of Geophysical Research: Solid Earth, 104/B8, 17661–17674. https://doi.org/10.1029/1999JB900120

Willett S.D., McCoy S.W., Perron J.T., Goren L., Chen C.-Y., 2014. Dynamic Reorganization of River Basins. Science, 343/6175, 1–9. https://doi.org/10.1126/science.1248765

Wobus C., Whipple K.X., Kirby E., Snyder N., Johnson J., Spyropolou K., Crosby B., Sheehan D., 2006. Tectonics from topography: Procedures, promise, and pitfalls. in Willett S.D., Hovius N., Brandon M.T., Fisher D.M., eds., Tectonics, Climate, and Landscape Evolution, Volume 398, Geological Society of America, pp. 55-74

Ziegler P.A., Dèzes P., 2007. Cenozoic uplift of Variscan Massifs in the Alpine foreland: Timing and controlling mechanisms. Global and Planetary Change, 58/1, 237–269. https://doi.org/10.1016/j.gloplacha.2006.12.004

Received: 27.09.2022
Accepted: 29.01.2023
Editorial Handling: Hugo Ortner